Interferon regulatory factor 2 binding protein 2b regulates neutrophil versus macrophage fate during zebrafish definitive myelopoiesis

Luxiang Wang, Shuo Gao, Haihong Wang, Chang Xue, Xiaohui Liu, Hao Yuan, Zixuan Wang, Saijuan Chen, Zhu Chen, Hugues de Thé, et al.

haematologica
Journal of The Ferrata Storti Foundation

Interferon regulatory factor 2 binding protein 2b regulates neutrophil versus macrophage fate during zebrafish definitive myelopoiesis

by Luxiang Wang, Shuo Gao, Haihong Wang, Chang Xue, Xiaohui Liu, Hao Yuan, Zixuan Wang, Saijuan Chen, Zhu Chen, Hugues de Thé, Yiyue Zhang, Wenqing Zhang, Jun Zhu, and Jun Zhou

Haematologica 2019 [Epub ahead of print]

Citation: Luxiang Wang, Shuo Gao, Haihong Wang, Chang Xue, Xiaohui Liu, Hao Yuan, Zixuan Wang, Saijuan Chen, Zhu Chen, Hugues de Thé, Yiyue Zhang, Wenqing Zhang, Jun Zhu, and Jun Zhou. Interferon regulatory factor 2 binding protein 2b regulates neutrophil versus macrophage fate during zebrafish definitive myelopoiesis.
Haematologica. 2019; 104:xxx
doi:10.3324/haematol.2019.217596

Interferon regulatory factor 2 binding protein 2b regulates neutrophil versus macrophage fate during zebrafish definitive myelopoiesis

Running head:

Irf2bp2b regulates zebrafish NMPs cell fate choice

*Luxiang Wang,[1] *Shuo Gao,[1] *Haihong Wang,[1] *Chang Xue,[1] Xiaohui Liu,[1] Hao Yuan,[1] Zixuan Wang,[1] Saijuan Chen,[1] Zhu Chen,[1] Hugues de Thé,[1,2] Yiyue Zhang,[3] Wenqing Zhang,[3] Jun Zhu,[1,2] and Jun Zhou,[1]

1 CNRS-LIA Hematology and Cancer, Sino-French Research Center for Life Sciences and Genomics, State Key Laboratory of Medical Genomics, Rui-Jin Hospital, Shanghai Jiao Tong University School of Medicine, Shanghai, P.R. China

2 Université de Paris 7/INSERM/CNRS UMR 944/7212, Equipe Labellisée No. 11 Ligue Nationale Contre le Cancer, Hôpital St. Louis, Paris, France

3. Division of Cell, Developmental and Integrative Biology, School of Medicine, South China University of Technology, Guangzhou 510006, P.R. China.

* These authors contributed equally to this work.

Contact information for correspondence: Dr. Jun Zhou, e-mail: zj10802@rjh.com.cn; or Dr. Jun Zhu, e-mail: zhuj1966@yahoo.com or jun.zhu@paris7.jussieu.fr; or Dr Wenqing Zhang, e-mail: mczhangwq@scut.edu.cn

Word count:

abstract: 193 words

main text: 4289 words

figures: 8

tables: 2

supplemental files: 1

Abstract

Proper cell fate choice of neutrophil-macrophage progenitor is essential for adequate myeloid sub-populations during embryonic development and in adulthood. The network governing neutrophil-macrophage progenitor cell fate is composed of several key determinants such as myeloid master regulators CCAAT enhancer binding protein alpha (C/EBPα) and spleen focus forming virus proviral integration oncogene (PU.1). Nevertheless, more regulators remain to be identified and characterized. To ensure balanced commitment of neutrophil-macrophage progenitor toward each lineage, the interplay among these determinants is not only synergistic, but also antagonistic. Depletion of Interferon regulatory factor 2 binding protein 2b (Irf2bp2b), a well known negative transcription regulator, results in a bias in neutrophil-macrophage progenitor cell fate choice which favors macrophages at the expense of neutrophils during the zebrafish definitive myelopoiesis stage in deficient embryos. Mechanistic studies indicate that Interferon regulatory factor 2 binding protein 2b acts as a downstream target of CCAAT enhancer binding protein alpha, to repress spleen focus forming virus proviral integration oncogene expression, and that SUMOylation confers the repressive function of Interferon regulatory factor 2 binding protein 2b. Thus, Interferon regulatory factor 2 binding protein 2b is a novel determinant in the cell fate choice of neutrophil-macrophage progenitor.

Introduction

Hematopoiesis is the process by which uncommitted hematopoietic stem cells (HSCs)

proliferate and differentiate into all mature blood cell types[1]. The stepwise development of multipotent HSCs undergoes sequential lineage potential limitations toward oligopotent and unipotent progenitor cells, eventually restrict their output[2]. The molecular network governing every stage of hematopoiesis involves the interplay between multiple lineage-specific transcription factors/cofactors and epigenetic modifiers[3]. Any tiny disturbance of these factors could bias the lineage-restricted cell fate toward an alternate fate[4].

Neutrophil-macrophage progenitors (NMPs) generate neutrophil macrophage lineage cells, mainly neutrophils, monocytes, and macrophages. The gene regulatory network (GRN) governing NMPs cell fate is composed of primary determinants C/EBPα and PU.1, along with secondary determinants Gfi and Egr/Nab[5, 6]. Neutrophil cell fate specification requires C/EBPα, whereas macrophage cell fate specification depends on PU.1[7, 8]. The relative levels of C/EBPα and PU.1 determines NMP cell fate choice. Low C/EBPα:PU.1 shifts the balance toward macrophage differentiation, whereas a high ratio directs granulocyte differentiation[6]. To keep myeloid lineage fidelity, the interplay among the determinants is important not only in initiating the differentiation toward one lineage, but also in inhibiting that of the other lineage. Gfi1 and Egr/Nab, the downstream transcription factors of C/EBPα and PU.1, function as mutual-antagonistic repressors to inhibit lineage-specific genes in mice[5, 9]. It has also been reported that the suppression of *irf8*, a downstream gene of Pu.1, leads to a depletion of macrophages and an expansion of neutrophils during zebrafish primitive myelopoiesis[10]. *Irf8* knockout mice even develop a chronic myeloid leukemia-like disease[11, 12]. Mechanistically, IRF8 impedes the ability of C/EBPα to stimulate neutrophil differentiation by preventing its binding to chromatin[12]. In addition to the transcription factors involved in C/EBPα and PU.1 network, Runx1 was shown to repress *pu.1* in a Pu.1-Runx1 negative feedback loop and determine the macrophage versus neutrophil fate[13].

IRF2BP2 is a member of the IRF2BP family that was initially identified as an interferon regulatory factor 2 (IRF2)-dependent corepressor in inhibiting the expression of interferon-responsive genes[14]. The IRF2BP family is highly conserved during evolution, and is structurally characterized by an N-terminal zinc finger motif which mediates homo- or hetero-dimerization/multimerization between different IRF2BP2 family members, and a C-terminal ring finger motif that interacts with its partners[15]. IRF2BP2 is described as a

corepressor in most published works[14, 16, 17]. The significance of IRF2BP2 in hematopoiesis was first revealed by genetic studies in *Irf2bp2*-deficient mice. IRF2BP2 acts with its binding partner ETO2, and the NCOR1/SMRT corepressor complex, to participate in erythroid differentiation[16]. As a ubiquitously distributed nuclear protein, IRF2BP2 plays multiple roles in various types of hematopoietic cells. For example, IRF2BP2 exerts a repressive function on nuclear factor of activated T cells (NFAT) target genes, which is another partner of IRF2BP2[17]. IRF2BP2 is also shown to restrain naive CD4 T cell activation by inhibiting proliferation and CD25 expression[18]. Moreover, *Irf2bp2*-deficient macrophages were inflammatory in mice[19]. In recent years, four acute promyelocytic leukemia (APL) patients carring a novel fusion IRF2BP2-RARα have been reported. Nevertheless, the potential role of IRF2BP2 in leukemogenesis is still unclear[20-23].

In this study, we provide *in vivo* evidence demonstrating that the deficiency of *irf2bp2b* triggers biased NMPs cell fate choice favoring macrophage development during zebrafish definitive myelopoiesis, which adds Irf2bp2b to the repertoire of factors regulating NMP cell fate decision. Mechanistic studies indicate that Irf2bp2b, which is under the control of C/ebpα, inhibits *pu.1* expression. We further reveal that SUMOylation is indispensable for the transcriptional repression of Irf2bp2b.

Methods

Zebrafish maintenance and mutant generation

Zebrafish were raised, bred, and staged according to standard protocols[24]. For crisp9 mediated *irf2bp2b* knockout zebrafish generation, guide RNA targeting exon1 of *irf2bp2b* was designed using an online tool ZiFiT Targeter software.

Plasmid construction

Zebrafish *irf2bp2b* gene and its serial mutants were cloned into $PCS2^{+}$ vector. The upstream sequences of zebrafish *pu.1*and *irf2bp2b* genes were cloned into PGL3 promoter vector (Promega). Primers used were listed in Table1.

Whole-mount in situ hybridization (WISH)

Digoxigenin-labeled RNA probes were transcribed with T7, T3 or SP6 polymerase (Ambion, Life Technologies, USA). WISH was performed as described previously[25].

Semiquantitative RT-PCR

The RNA preparation, cDNA synthesis, and quantitative RT-PCR were performed as described (Supplemental Methods).

Retroviral transduction

The IRF2BP2 cDNA was inserted into pMSCV-neo vector. For retroviral transduction, plat-E cells were transiently transfected with retroviral vectors. 32Dcl3 Cells were transduced by spinoculation (1,300 g, 30℃, 90 min) in a retroviral supernatant supplemented with cytokines and 4μg/ml polybrene (Sigma). Transduced cells were selected by G418 treatment (800mg/ml, Sigma).

Statistical analysis

For comparison of two means, statistical significance was evaluated by unpaired Student's t-test. For multiple comparisons, one-way analysis of variance (ANOVA) followed by LSD post hoc test for multiple comparisons. Differences were considered significant at $P<0.05$.

The animal protocol listed above has been reviewed and approved by the Animal Ethical and Welfare Committee, Rui-Jin Hospital, Shanghai Jiao Tong University School of Medicine, Shanghai, China.

Results

Deficiency of zebrafish *irf2bp2b* causes a reduction of the neutrophil population and a simultaneous expansion of the macrophage population in the definitive myelopoiesis stage

The *IRF2BP* gene family includes three members –*IRF2BP1*, *IRF2BP2* and *IRF2BPL*, which are highly conserved throughout evolution[15]. All the family members bear a nearly

identical N-terminal C4-type zinc finger motif and a C-terminal C3HC4-type ring finger motif, whereas the intermediate domain between the zinc finger and the ring finger motifs shows relatively low similarity at the protein level[15]. There are two paralog genes of *irf2bp2* named *irf2bp2a* and *irf2bp2b* in zebrafish, whereas a unique *IRF2BP2* gene exists in the human genome, which generates two isoforms also named *IRF2BP2a* and *IRF2BP2b* due to alternative splicing. Human IRF2BP2a has a sixteen amino acids long additional sequence in its intermediate domain compared with IRF2BP2b. Yet, this additional sequence in human IRF2BP2a is not conserved in zebrafish Irf2bp2a/2b (Figure S1). Phylogenetic analysis showed that the two paralogs and human *IRF2BP2* arose from a common ancestor, suggesting that functional divergence occurred early in vertebrate evolution[26].

The zebrafish is an excellent model organism for the study of hematopoiesis[27]. Like mammalian hematopoiesis, zebrafish hematopoiesis is also composed of primitive and definitive waves which emerge sequentially in distinct anatomical sites.

Human *IRF2BP2* mRNA is distributed in dozens of tissues, and the most prominent expression is found in bone marrow (https://www.ncbi.nlm.nih.gov/gene/359948). Zebrafish *irf2bp2b* is also ubiquitously expressed in developing embryos. *irf2bp2b* transcript was detected in the GFP positive cells enriched from Tg(*gata1*:eGFP), Tg(*pu.1*:eGFP), Tg(*mpx*:eGFP), and Tg(*mpeg1.1*:eGFP) embryos (Figure S2). To evaluate the effects of *irf2bp2b* on hematopoietic differentiation and lineage commitment, a mutant line was generated using the CRISPR/Cas9 system targeting the first exon of *irf2bp2b* gene and introduced a 26nt deletion which resulted in a truncated protein by frameshifting (Figure 1A-B). Moreover, the mutant *irf2bp2b* gene was cloned into an HA tagged expressing vector and transfected into HEK293T cells. As expected, a short protein was detected by western blot analysis. Meanwhile, immunofluorescence analysis showed that this Irf2bp2b mutant protein lost its nuclear localization due to loss of the NLS[28] (Figure 1C-D).

A series of hematopoietic related markers was detected by WISH analysis during the primitive hematopoiesis stage in *irf2bp2b*-defecient embryos. The primitive macrophages and neutrophils derived from the rostral blood island (RBI), as well as erythrocytes and neutrophils originating from intermediate cell mass (ICM) kept unchanged (Figure S3A-L, W).

Definitive pluripotent HSCs arise from the ventral wall of the dorsal aorta (VDA), the

zebrafish equivalent of the aorta/gonad/mesonephros (AGM) of mammals, then migrate through the caudal hematopoietic tissue (CHT) to the thymus and kidney marrow. WISH analyses revealed that the expression of the hematopoietic stem/progenitor cell (HSPC) related markers *runx1* and *c-myb* was relatively unchanged in *irf2bp2b*-defecient embryos (Figure S3M-R, X). In addition, the erythroid marker *hbαe1* (Figure S3S-T), and the lymphoid marker *rag1* (Figure S3U-V) were also unaffected.

As for myelopoiesis, a significant decrease in multiple neutrophil markers including *c/ebp1* (neutrophil progenitor marker)[29], *mpx*/*lyz* (mature neutrophil marker)[30] and a simultaneous increase of monocyte and macrophage markers like *csf1r* (monocyte/macrophage marker)[30], *mfap4*/*mpeg1.1* (early embryonic macrophage marker)[31, 32] were observed from 36 hours post fertilization (hpf) to 5 days post fertilization (dpf) in *irf2bp2b*-defecient mutants compared to controls (Figure 2A-I). The decreased neutrophil population was further confirmed by Sudan Black staining (SB)[33] at 3dpf in VDA (Figure 2J-J', M), as well as in *irf2bp2b*$^{-/-}$//Tg(*mpx*:eGFP) embryos at 5dpf in CHT (Figure 2K-K', M). Similarly, the expanded macrophage population was shown in *irf2bp2b*$^{-/-}$//Tg(*mpeg1.1*:eGFP) embryos at 5dpf (Figure 2L-L', M). Flow cytometry analysis was performed to quantify the numbers of neutrophils and macrophages, and the results showed a 34.9% reduction of eGFP positive cells in *irf2bp2b*$^{-/-}$//Tg(*mpx*:eGFP) embryos and a 21.4% increase in *irf2bp2b*$^{-/-}$//Tg(*mpeg1.1*:eGFP) embryos (Figure 2N-P). The *irf2bp2b*$^{-/-}$ zebrafish were not only viable but also fertile, which made the myelopoiesis study possible in the adults. Morphological staining of the three-month-old adult zebrafish kidney marrow further confirmed the expanded macrophages and reduced neutrophils (Figure 3A-C). Meanwhile, FACS analyses have also been done with the whole kidney marrows from Tg(*mpx*:eGFP) and *irf2bp2b*$^{-/-}$//Tg(*mpx*:eGFP) lines in three-month-old adults. The myeloid cells population were analyzed, and much less neutrophils were found in *irf2bp2b*$^{-/-}$//Tg(*mpx*:eGFP) zebrafish compared with controls (29.7% mpx^{+} vs 84.0% mpx^{+}) (Figure 3D, E).

A reverse phenotype emerged once *irf2bp2b* mRNA was injected in one-cell stage wild type embryos (Figure 3F-H). It is worth noting that the overall pan-myeloid marker *l-plastin*[30] positive cell numbers (which marks both the neutrophils and macrophages), were comparable among *irf2bp2b*-deficient mutants, *irf2bp2b* overexpressing and wild type embryos (Figure

3I-L). In addition, the embryos injected with specific *irf2bp2b* morpholino (MO) exactly phenocopied the aberrant myelopoiesis presented in *irf2bp2b* knockout embryos (Figure S4A-D, I).

All of the abnormalities in *irf2bp2b*-deficient and morphant embryos could be effectively rescued with the wild type zebrafish *irf2bp2b* mRNA, confirming the specificity of the phenotype (Figure S4E-F, I). Note that zebrafish *irf2bp2a* mRNA did not rescue the myelopoiesis defects, indicating the two paralogs might have distinct roles (data not shown). Accordingly, loss of *irf2bp2a* resulted in a quite different phenotype in zebrafish myelopoiesis, which could not be rescued by *irf2bp2b* mRNA, either (experiments ongoing). Moreover, human *IRF2BP2b* mRNA, but not *IRF2BP2a* mRNA, could rescue the biased myelopoiesis in zebrafish *irf2bp2b*-defecient mutants, suggesting human *IRF2BP2b* should be the functional ortholog of zebrafish *irf2bp2b* in this process (Figure S4G-H, I, and data not shown).

Irf2bp2b regulates NMP cell fate choice by repressing *pu.1* expression

The imbalanced proportion of neutrophil and macrophage populations in *irf2bp2b*-defective mutants can result from either abnormalities in apoptosis or proliferation rate. To distinguish between these possibilities, TUNEL and antiphosphohistone H3 (pH3) antibody staining assays were performed to assess the apoptosis and proliferation status of neutrophils and macrophages, respectively. Neither TUNEL nor pH3 assays displayed a discernable change in the percentage of double positive stained cells ($TUNEL^{+}GFP^{+}$, $pH3^{+}GFP^{+}$) within *irf2bp2b*$^{-/-}$//Tg(*mpx*:eGFP) and *irf2bp2b*$^{-/-}$//Tg(*mpeg1*:eGFP) embryos compared to controls, indicating that there is no change in either the apoptosis or proliferation status of each lineage in *irf2bp2b*-deficient embryos (Figure S5). Moreover, the fact that *l-plastin* positive cell numbers remained unchanged in both *irf2bp2b* overexpressing and deficient embryos suggested that *irf2bp2b* might participate in regulating neutrophil versus macrophage fate choice.

The relative level of the master regulators PU.1 and C/EBPα is critical in macrophage versus neutrophil cell fate specification[6]. To ensure a balanced commitment of NMPs, the endogenous levels of PU.1 and C/EBPα must be appropriately tuned to a proper range. Overexpression of PU.1 can bias myeloid output to macrophage fate, whereas overexpression

of C/EBPα exerts a reverse function. Thus either *pu.1*upregulation or *c/ebpα* downregulation within NMPs could be causative of the biased myelopoiesis toward macrophages in *irf2bp2b* mutants. Firstly we tried to examine the expression levels of *pu.1* and *c/ebpα* by WISH analysis. Unfortunately, no obvious difference could be observed between the wild type and *irf2bp2b*$^{-/-}$ embryos. Considering that *Pu.1* is expressed in multiple hematopoietic cell lineages such as the HSCs, the common lymphoid progenitors, and the common myeloid progenitors[34], and *C/ebpα* is also widely expressed in HSCs and myeloid cells[35], the changes of their expression levels within NMP might be difficult to be shown. Due to the lack of a lineage cell detection cocktail for the zebrafish hematopoietic system, we were unable to isolate the NMP subpopulation by flow cytometry to compare the endogenous expression levels of *pu.1*and *c/ebpα*. Quantitative reverse transcription PCR (RT-qPCR) was performed to detect the expression of *c/ebpα* and *pu.1* in wild type and *irf2bp2b*-defecient whole embryos, and no obvious change could be observed (Figure S6), suggesting that the change occurred in NMPs might be masked. To resolve this problem, we used a murine myeloid progenitor cell line 32Dcl3 retrovirally transduced with human *IRF2BP2b*. RT-qPCR analyses revealed that the transcript level of *Pu.1* was downregulated, whereas that of *C/ebpα* was unaffected (Figure 4A). Meanwhile, expression of multiple monocyte differentiation-related genes such as *Mcsfr*, *Mmp1*, *Tlr2*, and *Irf8* were reduced, whereas expression of neutrophil differentiation-related genes like *Gcsfr*, *Ltf*, *Prtn3*, and *Elane* were induced (Figure 4A). This observation implies that the alteration of *pu.1* expression, rather than that of *c/ebpα*, might account for the balance shift of neutrophil and macrophage populations in *irf2bp2b*-deficient zebrafish embryos. Since IRF2BP2 is a negative transcription regulator, we wondered whether *pu.1* is a direct target of Irf2bp2b, which could be upregulated in *irf2bp2b*-deficient NMPs. To test this hypothesis, we divided the 8.5kb zebrafish *pu.1* promoter into four fragments, which were inserted separately into a luciferase reporter vector[13]. The luciferase expression in all of these four constructs was inhibited when co-transfected with *irf2bp2b* in HEK293T cells. The most prominent repression was found within the fragment nearest to transcription start site (-1.7kb) (Figure 4B). Next, a series of *in vivo* experiments was performed. The 8.5kb *pu.1* promoter was cloned into a mCherry reporter vector (*pu.1*:mCherry, Tol2 backbone), which was co-injected with Tol2 transposase mRNA into wild type zebrafish embryos with or without *irf2bp2b* mRNA.

Overexpression of *irf2bp2b* led to a significantly reduced expression of mCherry (Figure 4C-D). Moreover, *pu.1* MO was injected into *irf2bp2b*$^{-/-}$ embryos, and an effective rescue effect of aberrant myelopoiesis was obtained (Figure 4E-J, O). These observations suggested that *pu.1* expression level might be elevated within NMPs in *irf2bp2b* mutants. To further demonstrate that Irf2bp2b regulates zebrafish NMP cell fate choice through repression of *pu.1*, we took advantage of a zebrafish *pu.1*^{G242D} mutant line, in which *pu.1* transcripts level is normal but its protein stability is dramatically decreased[13]. In *pu.1*$^{G242D/G242D}$ homozygous embryos, biased myelopoiesis toward neutrophils appeared as expected. Note that no obvious rescue effect was observed in the *irf2bp2b*$^{-/-}$*pu.1*$^{G242D/G242D}$ double-mutant embryos compared to *pu.1*$^{G242D/G242D}$ embryos, indicating that *pu.1* is indeed the downstream of Irf2bp2b in determining NMP cell fate (Figure 4K-O).

Irf2bp2b represses *pu.1* gene transcription by directly binding to its promoter

IRF2BP2 was frequently described as a corepressor[14, 16, 17]. We then set out to investigate how Irf2bp2b represses *pu.1* expression. The C-terminal C3HC4-type ring finger motif of IRF2BP2 is responsible for mediating the binding with its interacting partners[14, 16, 17]. The role of the N-terminal C4-type zinc finger motif was believed to enable the homo and hetero-dimerization/multimerization between different IRF2BP2 family members[15]. However, C4 zinc fingers are typically found in DNA binding domains (DBDs) of transcription factors including GATA1-6 as well as nuclear receptors RAR and RXR[36, 37]. Therefore, the possibility that IRF2BP2 functions as a transcription repressor by directly binding DNA should not be excluded.

To characterize how Irf2bp2b represses transcription in NMP cell fate choice, a series of point mutations in critical cysteines were introduced into the ring finger (C420/423A, named RM thereafter) and the zinc finger motif (C14/17A, named ZM thereafter) of Irf2bp2b as previously reported[15] (Figure 5A). For the Irf2bp2b RM mutant, interaction with its partners was abolished, while the polymerization and the putative DNA binding capacities of the ZM mutant were both abrogated. A tetramerization motif from human P53 (amino acids 324-355) was fused in frame with the Irf2bp2b ZM mutant (tet-ZM), restoring the polymerization capacity of this mutant (Figure 5A). Immunofluorescence analysis (anti-HA antibody) of

HEK293T cells transfected with the Irf2bp2b mutants described above demonstrated these mutations did not affect nuclear localization as expected (Figure S7) [28].

The results from *in vivo* rescue assays revealed that only the RM mutant displayed a significant rescue effect similar to wild type *irf2bp2b*, whilst the ZM and tet-ZM mutants did not (Figure 5B-L). These data indicate that direct DNA binding would be indispensable for ability of Irf2bp2b to repress *pu.1* gene expression in NMP cell fate choice.

Correspondingly, the luciferase activity assays showed that only wild type Irf2bp2b and RM mutant, but not ZM and tet-ZM mutants, exhibited strong repression effects on luciferase expression with a -1.7kb zebrafish *pu.1* promoter (Figure 6A). This fragment was further narrowed down to a short 132bp region (A region) (Figure 6B). To validate that the A region is an Irf2bp2b binding site, an *in vivo* chromatin immunoprecipitation PCR (CHIP-PCR) was performed in zebrafish embryos expressing GFP or Irf2bp2b-GFP using an anti-GFP antibody. Using the assay, the *pu.1* promoter A region was specifically co-immunoprecipitated (co-IP) with Irf2bp2b-GFP (Figure 6C).

Since positively charged amino acids are important to fit into the negatively charged phosphate backbone of DNA, several arginines (R10/11/36/55/59) within the C4 zinc finger motif were mutated. Luciferase assays showed that only the Irf2bp2b$^{R55/59L}$ double-mutant completely lost the ability to repress luciferase expression from the *pu.1* promoter (Figure 6D). Notably, CHIP-PCR analysis has shown that Irf2bp2b$^{R55/59L}$ mutant could not co-immunoprecipitate the *pu.1* promoter A region (Figure 6C). As anticipated, this mutant lost the rescue effect in *irf2bp2b*$^{-/-}$ embryos (Figure 6E-J, K). These results indicate that Irf2bp2b represses *pu.1* gene expression by directly binding to its promoter and R55/R59 are two critical amino acids for Irf2bp2b DNA binding.

Taken together, these findings suggest that Irf2bp2b functions most likely as a transcription repressor, rather than a corepressor, in NMPs fate choice during zebrafish myelopoiesis.

Repression property of Irf2bp2b is SUMOylation dependent

IRF2BP2 is a corepressor molecule for its interacting transcription factors[14, 17]. In the current study, we demonstrated that zebrafish Irf2bp2b inhibits *pu.1* expression. Thus, we

investigated the reason underlying the repression property of IRF2BP2.

Protein post-translational modification (PTM) plays a pivotal role in regulating function. SUMOylation is an important type of PTM which involves a cascade of dedicated enzymes that facilitate the covalent modification of specific lysine residues on target proteins with monomers or polymers of SUMO (Small Ubiquitin-like Modifier)[38]. The SUMOylation of substrate proteins is frequently linked with transcriptional repression[39]. Actually, multiple adducts (the smallest one was about 10kD larger than the unmodified protein, which was nearly the size of one SUMO molecule) of Irf2bp2b were detected by western blot (Figure 7A). The SUMO-targeted lysine usually lies in the canonical motif ψKXE[40]. A SUMO consensus motif VKKE (lysine 496) located at the C-terminus of Irf2bp2b was predicted by bioinformatics (Figure S1). The putative lysine was mutated to arginine (Irf2bp2b^{K496R}) to abolish covalent binding with the SUMO molecule. The modified bands of the Irf2bp2b^{K496R} mutant protein disappeared as expected (Figure 7A-B). In addition, an Irf2bp2b^{E498A} mutant was constructed to destroy the conservation of the SUMO consensus motif which still allowing the accessibility of the lysine 496 to other modifiers. The modified bands disappeared as Irf2bp2b ^{K496R} mutant did (Figure 7C), indicating Irf2bp2b is a SUMOylated substrate.

In HEK293T cells, GFP-SUMO was cotransfected with HA-tagged wild type Irf2bp2b or Irf2bp2b^{K496R} mutant. Immunoprecipitation (IP) assays showed that GFP-SUMO co-precipitated with HA-tagged wild type Irf2bp2b, but not with the Irf2bp2b^{K496R} mutant (Figure 7D). This further indicated that Irf2bp2b is indeed SUMOylated in cells.

Luciferase reporter assays with zebrafish *pu.1* promoter were then conducted to assess Irf2bp2b repression capacity upon its SUMOylation. Results have shown that Irf2bp2b-SUMO fusion which mimics fully SUMOylated Irf2bp2b displayed an even stronger repression than wild type Irf2bp2b, whereas Irf2bp2b^{K496R} mutant lost the ability to repress transcription (Figure 7B, E). Consistently, Irf2bp2b-SUMO and Irf2bp2b^{K496R} mutants performed completely different rescue effects in *irf2bp2b*-defecient mutants (Figure 7F-N).

Overall, these data supported that Irf2bp2b is a SUMOylated protein in cells and SUMOylation is indispensable for its transcription repression property.

Irf2bp2b mediates the antagonistic effect of C/ebpα on *pu.1* in NMPs cell fate choice

To ensure balanced commitment of NMPs toward each lineage, the mutual antagonistic interplay of the master regulators PU.1 and C/EBPα is very important[5, 41]. Since Irf2bp2b represses *pu.1* expression in zebrafish NMPs cell fate choice, we then raised the question whether *irf2bp2b* is a C/ebpα target.

Two putative C/ebpα binding sites located at -37bp (CS1) and -1595bp (CS2) upstream of the transcription start site were predicted in the zebrafish *irf2bp2b* promoter by bioinformatics analysis. A luciferase reporter vector was constructed with the zebrafish *irf2bp2b* -2.2kb promoter and cotransfected with either a *c/ebpα* expressing vector or an empty vector. Luciferase expression was significantly enhanced by C/ebpα (Figure 8A). Similar expression enhancement was also obtained when an mCherry expressing vector carrying the same *irf2bp2b* promoter (*irf2bp2b*:mCherry, in Tol2 backbone) was co-injected with *c/ebpα* and Tol2 transposase mRNAs into zebrafish embryos (Figure 8B-C). This enhancement was completely abolished when the predicted C/ebpα binding sites were deleted in the *irf2bp2b* promoter (Figure 8D).

Finally, *c/ebpα* mRNA was injected into *irf2bp2b*$^{-/-}$ knockout and wild type embryos, respectively. The overexpression of *c/ebpα* mRNA induced biased myelopoiesis toward neutrophils in control embryos (Figure 8E-F, I-J, M), but had no effect on myelopoiesis in *irf2bp2b*$^{-/-}$ embryos (Figure 8G-H, K-M).

Meanwhile, to elucidate whether *gfi1* could also be a secondary determinant of C/ebpα, *gfi1* mRNA was injected into wild type embryos. Although *gfi1* overexpression did give rise to a remarkable expansion of the neutrophil population, the macrophage population was unaffected (data not shown). Moreover, such overexpression did not display any rescue effect in *irf2bp2b*-deficient embryos (Figure S8E-F, I).

In summary, these data indicate that Irf2bp2b plays a pivotal role in mediating the antagonistic function of C/ebpα on *pu.1* transcription regulation, which fine tunes the *pu.1* expression level in NMPs and determines NMPs cell fate choice in order to maintain a normal neutrophil and macrophage population ratio (Figure 8N).

Discussion

Although multiple regulators involved in hematopoietic lineage restriction have been characterized, the molecular details of NMP differentiation are still under debate. The relationship between the master regulators PU.1 and C/EBPα in myelopoiesis is complicated, which is not only synergistic, but also antagonistic[41]. On one side, C/EBPα can stimulate *PU.1* expression by directly binding to its promoter[42, 43]. On the other side, C/EBPα can directly interact with PU.1 and block its function, or inhibit *PU.1* indirectly through activation of the transcription repressor *GFI1*[44, 45], which in turn inhibits PU.1 activity through protein-protein interaction[46]. In the present study, we determined that in the balance between granulocytic and macrophagic commitment, zebrafish *irf2bp2b* acts as a direct target of C/ebpα to repress *pu.1* expression. Our data also suggest that during definitive myelopoiesis stage of zebrafish, it is the C/ebpα-Irf2bp2b-Pu.1 axis, not C/ebpα-Gfi1-Pu.1, that regulates NMP cell fate choice. Thus zebrafish Irf2bp2b acts as a novel player in NMP cell fate decision and adds a new layer of complexity to this fine-tuning process.

Note that in *irf2bp2b*-defecient embryos the primitive macrophages and neutrophils developed normally (Figure S3C-D, G-H, K-L). Previously it has been reported that a Pu.1-Runx1 negative feedback loop determines the RBI-originated macrophage versus neutrophil fate[13]. Runx1 was shown to directly inhibit the *pu.1* promoter in the study, however, injection of *runx1* mRNA into our *irf2bp2b*-defecient embryos could not rescue the aberrant myelopoiesis (Figure S8G-I). To further elucidate whether *irf2bp2b* regulates primitive myeloid differentiation, we first determined *irf2bp2b* is present in primitive versus definitive progenitor cells (Figure S9A). Then we injected *irf2bp2b* mRNA into one-cell stage wild type embryos. The biased myelopoiesis could only be observed in VDA at 48hpf (Fig 3F-H). By contrast, *c/ebp1*, *lyz*, and *mfap4* were all normally expressed in RBI at 22hpf (Fig S9B-H). Based on these observations, we believe that even though *irf2bp2b* is expressed in both primitive and definitive myeloid progenitor cells, distinct regulatory mechanisms are implicated in cell fate determination of NMPs derived from VDA/CHT and RBI.

The DNA binding properties of IRF2BP2 has never been studied. Although C4-type zinc fingers are found in Irf2bp2, GATA, RARα, and RXR, there are still some differences. While a single C-X2-C-X17-C-X2-C type zinc finger exists in Irf2bp2, two consecutive ones are

contained in GATA. RARα and RXR have two C-X2-C-X13-C-X2-C type zinc fingers. GATA binds specifically to consensus sequence[47]. Physiologically RAR-RXR heterodimer binds to responsive elements that consist of two AGGTCA core motifs[48]. To find out the binding site of Irf2bp2b within the *pu.1* promoter, we first wondered whether it was similar to that of GATA or RAR/RXR. Two putative GATA binding sites (GS1, GS2) were predicted within the 132bp A region, whereas no RAR/RXR binding sites could be found. However, both GATA site deletion constructs could still be inhibited by Irf2bp2b (Figure S10). Therefore, Irf2bp2b presumably has its own binding site.

The majority of APL patients bear a PML-RARα fusion gene. However, in APL variants RARα is fused with genes other than PML. Recently, four APL cases with a novel fusion, IRF2BP2-RARα, were identified[20-23]. All X-RARα fusion related APL is characterized by the blockage at the promyelocyte stage and the inhibition of a large set of differentiation related genes targeted by corepressors recruited onto RARα moiety[49]. Note that the zinc finger motif of IRF2BP2 is intact in all of the four patients carrying the IRF2BP2-RARα oncoprotein[20-23], thus two potential DBDs from each moiety are retained simultaneously in the fusion. Such a phenomenon is very rare in a chimeric fusion protein composed of two transcription factors. This raises a few questions about IRF2BP2-RARα related APL. Since dimerization is one of a prerequisite for all X-RARα fusions[50], does the IRF2BP2 moiety serves merely as an interface for dimerization of IRF2BP2-RARα, or does IRF2BP2 have other contributions, such as DNA binding, in APL pathogenesis? Does IRF2BP2-RARα arise at NMP level? If it is expressed in NMPs, whether IRF2BP2-RARα could trigger the biased NMPs cell fate choice favoring granulopoiesis? Further studies are needed to answer these questions.

Acknowledgments

The authors are grateful to Y Chen and J Jin (both from Shanghai Jiao Tong University School of Medicine, Shanghai, China) for technical support. We thank Dr. X Jiao, Dr. Maria Mateyak, and Dr. Sunny Sharma (all from Department of Cell Biology and Neuroscience, Rutgers University, Piscataway, NJ 08854, USA) for their critical manuscript reading.

This work was supported by research funding from the National Natural Science Foundation of China (31871471).

Authorship Contributions

L.W., S.G., H.W., C.X., X.L., H.Y., and Z.W performed experiments, and analyzed data; Y.Z and W.Z. provided critical experiment materials; Z.C., H.T., S.C., J.Z., and J.Z participated in the preparation of manuscript; J.Z and J.Z designed the research and analyzed data.

Conflict of Interest

The authors declare no competing financial interests.

References

1. Evans T. Developmental biology of hematopoiesis. Hematol Oncol Clin North Am. 1997;11(6):1115-1147.
2. Carrelha J, Meng Y, Kettyle LM, et al. Hierarchically related lineage-restricted fates of multipotent haematopoietic stem cells. Nature. 2018;554(7690):106-111.
3. Gottgens B. Regulatory network control of blood stem cells. Blood. 2015;125(17):2614-2620.
4. Yuan H, Zhou J, Deng M, et al. Sumoylation of CCAAT/enhancer-binding protein alpha promotes the biased primitive hematopoiesis of zebrafish. Blood. 2011;117(26):7014-7020.
5. Laslo P, Spooner CJ, Warmflash A, et al. Multilineage transcriptional priming and determination of alternate hematopoietic cell fates. Cell. 2006;126(4):755-766.
6. Dahl R, Walsh JC, Lancki D, et al. Regulation of macrophage and neutrophil cell fates by the PU.1:C/EBPalpha ratio and granulocyte colony-stimulating factor. Nat Immunol. 2003;4(10):1029-1036.
7. Zhang DE, Zhang P, Wang ND, Hetherington CJ, Darlington GJ, Tenen DG. Absence of granulocyte colony-stimulating factor signaling and neutrophil development in CCAAT enhancer binding protein alpha-deficient mice. Proc Natl Acad Sci U S A. 1997;94(2):569-574.
8. Scott EW, Simon MC, Anastasi J, Singh H. Requirement of transcription factor PU.1 in the development of multiple hematopoietic lineages. Science. 1994;265(5178):1573-1577.
9. Hock H, Hamblen MJ, Rooke HM, et al. Intrinsic requirement for zinc finger transcription factor Gfi-1 in neutrophil differentiation. Immunity. 2003;18(1):109-120.
10. Li L, Jin H, Xu J, Shi Y, Wen Z. Irf8 regulates macrophage versus neutrophil fate during zebrafish primitive myelopoiesis. Blood. 2011;117(4):1359-1369.
11. Tamura T, Kurotaki D, Koizumi S. Regulation of myelopoiesis by the transcription factor IRF8. Int J Hematol. 2015;101(4):342-351.
12. Kurotaki D, Yamamoto M, Nishiyama A, et al. IRF8 inhibits C/EBPalpha activity to restrain mononuclear phagocyte progenitors from differentiating into neutrophils. Nat Commun. 2014;5:4978.
13. Jin H, Li L, Xu J, et al. Runx1 regulates embryonic myeloid fate choice in zebrafish through a negative feedback loop inhibiting Pu.1 expression. Blood. 2012;119(22):5239-5249.
14. Childs KS, Goodbourn S. Identification of novel co-repressor molecules for Interferon Regulatory Factor-2. Nucleic Acids Res. 2003;31(12):3016-3026.
15. Yeung KT, Das S, Zhang J, et al. A novel transcription complex that selectively modulates apoptosis of breast cancer cells through regulation of FASTKD2. Mol Cell Biol. 2011;31(11):2287-2298.

16. Stadhouders R, Cico A, Stephen T, et al. Control of developmentally primed erythroid genes by combinatorial co-repressor actions. Nat Commun. 2015;6:8893.

17. Carneiro FR, Ramalho-Oliveira R, Mognol GP, Viola JP. Interferon regulatory factor 2 binding protein 2 is a new NFAT1 partner and represses its transcriptional activity. Mol Cell Biol. 2011;31(14):2889-2901.

18. Secca C, Faget DV, Hanschke SC, et al. IRF2BP2 transcriptional repressor restrains naive CD4 T cell activation and clonal expansion induced by TCR triggering. J Leukoc Biolo. 2016;100(5):1081-1091.

19. Chen HH, Keyhanian K, Zhou X, et al. IRF2BP2 Reduces Macrophage Inflammation and Susceptibility to Atherosclerosis. Circ Res. 2015;117(8):671-683.

20. Yin CC, Jain N, Mehrotra M, et al. Identification of a novel fusion gene, IRF2BP2-RARA, in acute promyelocytic leukemia. J Natl Compr Canc Netw. 2015;13(1):19-22.

21. Shimomura Y, Mitsui H, Yamashita Y, et al. New variant of acute promyelocytic leukemia with IRF2BP2-RARA fusion. Cancer Sci. 2016;107(8):1165-1168.

22. Jovanovic JV, Chillon MC, Vincent-Fabert C, et al. The cryptic IRF2BP2-RARA fusion transforms hematopoietic stem/progenitor cells and induces retinoid-sensitive acute promyelocytic leukemia. Leukemia. 2017;31(3):747-751.

23. Mazharuddin S, Chattopadhyay A, Levy MY, Redner RL. IRF2BP2-RARA t(1;17)(q42.3;q21.2) APL blasts differentiate in response to all-trans retinoic acid. Leuk Lymphoma. 2018;59(9):2246-2249.

24. Kimmel CB, Ballard WW, Kimmel SR, Ullmann B, Schilling TF. Stages of embryonic development of the zebrafish. Dev Dyn. 1995;203(3):253-310.

25. Thisse C, Thisse B. High-resolution in situ hybridization to whole-mount zebrafish embryos. Nat Protoc. 2008;3(1):59-69.

26. Teng AC, Kuraitis D, Deeke SA, et al. IRF2BP2 is a skeletal and cardiac muscle-enriched ischemia-inducible activator of VEGFA expression. FASEB J. 2010;24(12):4825-4834.

27. Gore AV, Pillay LM, Venero Galanternik M, Weinstein BM. The zebrafish: A fintastic model for hematopoietic development and disease. Wiley Interdiscip Rev Dev Biol. 2018;7(3):e312.

28. Teng AC, Al-Montashiri NA, Cheng BL, et al. Identification of a phosphorylation-dependent nuclear localization motif in interferon regulatory factor 2 binding protein 2. PloS One. 2011;6(8):e24100.

29. Lekstrom-Himes J, Xanthopoulos KG. CCAAT/enhancer binding protein epsilon is critical for effective neutrophil-mediated response to inflammatory challenge. Blood. 1999;93(9):3096-3105.

30. Meijer AH, van der Sar AM, Cunha C, et al. Identification and real-time imaging of a myc-expressing neutrophil population involved in inflammation and mycobacterial granuloma formation in zebrafish. Dev Comp Immunol. 2008;32(1):36-49.

31. Zakrzewska A, Cui C, Stockhammer OW, Benard EL, Spaink HP, Meijer AH. Macrophage-specific gene functions in Spi1-directed innate immunity. Blood. 2010;116(3):e1-11.

32. Spilsbury K, O'Mara MA, Wu WM, Rowe PB, Symonds G, Takayama Y. Isolation of a novel macrophage-specific gene by differential cDNA analysis. Blood. 1995;85(6):1620-1629.

33. Le Guyader D, Redd MJ, Colucci-Guyon E, et al. Origins and unconventional behavior of neutrophils in developing zebrafish. Blood. 2008;111(1):132-141.

34. Nutt SL, Metcalf D, D'Amico A, Polli M, Wu L. Dynamic regulation of PU.1 expression in multipotent hematopoietic progenitors. J Exp Med. 2005;201(2):221-231.

35. Avellino R, Delwel R. Expression and regulation of C/EBPalpha in normal myelopoiesis and in malignant transformation. Blood. 2017;129(15):2083-2091.

36. Vonderfecht TR, Schroyer DC, Schenck BL, McDonough VM, Pikaart MJ. Substitution of DNA-contacting amino acids with functional variants in the Gata-1 zinc finger: a structurally and phylogenetically guided

mutagenesis. Biochem Biophys Res Commun. 2008;369(4):1052-1056.

37. Urnov FD. A feel for the template: zinc finger protein transcription factors and chromatin. Biochem Cell Biol. 2002;80(3):321-333.

38. Han ZJ, Feng YH, Gu BH, Li YM, Chen H. The post-translational modification, SUMOylation, and cancer (Review). Int J Oncol. 2018;52(4):1081-1094.

39. Garcia-Dominguez M, Reyes JC. SUMO association with repressor complexes, emerging routes for transcriptional control. Biochim Biophys Acta. 2009;1789(6-8):451-459.

40. Rodriguez MS, Dargemont C, Hay RT. SUMO-1 conjugation in vivo requires both a consensus modification motif and nuclear targeting. J Biol Chem. 2001;276(16):12654-12659.

41. Weston BR, Li L, Tyson JJ. Mathematical Analysis of Cytokine-Induced Differentiation of Granulocyte-Monocyte Progenitor Cells. Front Immunol. 2018;9:2048.

42. Kummalue T, Friedman AD. Cross-talk between regulators of myeloid development: C/EBPalpha binds and activates the promoter of the PU.1 gene. J Leukoc Biol. 2003;74(3):464-470.

43. Yeamans C, Wang D, Paz-Priel I, Torbett BE, Tenen DG, Friedman AD. C/EBPalpha binds and activates the PU.1 distal enhancer to induce monocyte lineage commitment. Blood. 2007;110(9):3136-3142.

44. Lidonnici MR, Audia A, Soliera AR, et al. Expression of the transcriptional repressor Gfi-1 is regulated by C/EBP{alpha} and is involved in its proliferation and colony formation-inhibitory effects in p210BCR/ABL-expressing cells. Cancer Res. 2010;70(20):7949-7959.

45. Reddy VA, Iwama A, Iotzova G, et al. Granulocyte inducer C/EBPalpha inactivates the myeloid master regulator PU.1: possible role in lineage commitment decisions. Blood. 2002;100(2):483-490.

46. Dahl R, Iyer SR, Owens KS, Cuylear DD, Simon MC. The transcriptional repressor GFI-1 antagonizes PU.1 activity through protein-protein interaction. J Biol Chem. 2007;282(9):6473-6483.

47. Trainor CD, Omichinski JG, Vandergon TL, Gronenborn AM, Clore GM, Felsenfeld G. A palindromic regulatory site within vertebrate GATA-1 promoters requires both zinc fingers of the GATA-1 DNA-binding domain for high-affinity interaction. Mol Cell Biol. 1996;16(5):2238-2247.

48. de The H, Vivanco-Ruiz MM, Tiollais P, Stunnenberg H, Dejean A. Identification of a retinoic acid responsive element in the retinoic acid receptor beta gene. Nature. 1990;343(6254):177-180.

49. de The H, Pandolfi PP, Chen Z. Acute Promyelocytic Leukemia: A Paradigm for Oncoprotein-Targeted Cure. Cancer Cell. 2017;32(5):552-560.

50. Zhou J, Peres L, Honore N, Nasr R, Zhu J, de The H. Dimerization-induced corepressor binding and relaxed DNA-binding specificity are critical for PML/RARA-induced immortalization. Proc Nal Acad Sci U S A. 2006;103(24):9238-9243.

Figure legends

Figure 1. The establishment of a zebrafish *irf2bp2b* knock out line. (A) Schematic representation of Cas9 target site in the first exon of zebrafish *irf2bp2b*. The deleted nucleotides in the mutant gene are marked by hyphens. (B) Schematic representation of wild type (501 amino acids) and mutant Irf2bp2b proteins (201 amino acids). The site where the frameshift was introduced is marked by triangles. (C) Western blot analysis of HA-tagged wild type and mutant Irf2bp2b proteins. (D) Immunofluorescence analysis of wild type (top panel) and mutant Irf2bp2b (bottom panel) proteins, demonstrating that the truncated protein lost its nuclear localization.

Figure 2. Deficiency of *irf2bp2b* leads to an expanded macrophage population at the expense of the neutrophil population during definitive myelopoiesis. (A-D') WISH analyses of neutrophil markers *c/ebp1* (A, A'), *mpx* (B-C'), and *lyz* (D, D') at 36hpf, 48hpf, and 5dpf in wild type (WT) and *irf2bp2b*-deficient embryos, respectively. Grey boxes and red arrows indicate the main position of positive cells for each marker. n/n, number of embryos showing representative phenotype/total number of embryos examined. (E-H') WISH analyses of monocytes/macrophages markers *csf1r* (E, E'), *mpeg1.1* (F, F'), and *mfap4* (G-H') at 48hpf and 5dpf. (I) Statistical results for A-H'. Error bars represent ± SD of at least 15-30 embryos. p values are denoted by asterisks; (***)P<0.001 (Student's t test). (J, J') Sudan Black positive cells are reduced in *irf2bp2b*-deficient embryos at 3dpf. (K, K') GFP positive cells are decreased in *irf2bp2b*$^{-/-}$//Tg(*mpx*:eGFP) embryos at 5dpf. (L, L') GFP positive cells increased in *irf2bp2b*$^{-/-}$//Tg(*mpeg1.1*:eGFP) embryos at 5dpf. (M) Statistical results for J-L'. (***)P<0.001; (****)P<0.0001 (Student's t test). (N, O) FACS Analysis of eGFP positive cells in wild type and *irf2bp2b*$^{-/-}$//Tg(*mpx*:eGFP) or *irf2bp2b*$^{-/-}$//Tg(*mpeg1.1*:eGFP) embryos at 2dpf. (P) Statistical results for N, O. Error bars represent ± SD of 3 replicates. (**) P<0.01; (***) P<0.001 (Student's t test).

Figure 3. Biased myelopoiesis in *irf2bp2b*-deficient adult zebrafish. (A, B) HE staining morphological analysis of the kidney marrow collected from the three-month-old adult wild type (one male and one female) and *irf2bp2b*$^{-/-}$ (two males and one female) zebrafish. One

representative image of each group was shown. Green and red arrows indicated the typical neutrophils and macropahges, respectively. (C) Statistical results for A, B. Error bars represent ± SD of at least 15 images. (***) P<0.001 (Student's t test). (D) FACS analysis of whole kidney marrows from Tg(*mpx*:eGFP) and *irf2bp2b*$^{-/-}$//Tg(*mpx*:eGFP) lines in three-month-old adults. The myeloid cells within R5 gate were analyzed with fluorescence. (E) Statistical results for D. Error bars represent ± SD of 3 replicates. (****) P<0.0001 (Student's t test). (F-G') *Mpx* and *mfap4* were used to monitor neutrophils and macrophages development in wild type and *irf2bp2b* mRNA injected embryos by WISH. (I-K) WISH analyses of pan-myeloid marker *l-plastin* of wild type, *irf2bp2b*$^{-/-}$, and *irf2bp2b* mRNA injected embryos. (H, L) Statistical results for F-G', I-K. Error bars represent ± SD of at least 15-30 embryos. p values are denoted by asterisks; (ns): no statistical significance; (**) P<0.01; (***) P<0.001 (Student's t test).

Figure 4**. Irf2bp2b dictates NMP cell fate through inhibition of *pu.1*expression.** (A) RT-qPCR analysis of neutrophil and macrophage development related genes in 32Dcl3 cells constitutively expressing human *IRF2BP2b*. Error bars represent ± SD of at least 3 replicates. p values are denoted by asterisks; (ns): no statistical significance; (**)P<0.01; (***)P<0.001 (Student's t test). (B) Schematic diagram of the -8.5kb zebrafish *pu.1* promoter dual luciferase report vector (top panel). Dual Luciferase vectors each with a fragment of the zebrafish *pu.1* promoter as indicated were cotransfected into HEK293T cells with an *irf2bp2b* expressing vector or empty vector pCS2^{+}. Luciferase activity with *irf2bp2b* expression was detected and normalized to empty vector pCS2^{+} which was set to 1.0 (bottom panel). Error bars represent ± SD of at least 3 replicates. p values are denoted by asterisks; (***)P<0.001; (****)P<0.0001 (Student's t test). (C, D) Representative fluorescent images of transient mCherry expression at 48hpf of WT and *irf2bp2b* overexpressing embryos injected with a -8.5kb *pu.1*:mCherry construct. (E-N) WISH assay of *mpx* and *mfap4* in WT (E, F), *irf2bp2b*$^{-/-}$ mutant embryos (G, H), *irf2bp2b*$^{-/-}$ mutant embryos injected with *pu.1* MO (I, J), *pu.1*$^{G242D/G242D}$ mutants (K, L), and *irf2bp2b*$^{-/-}$*pu.1* $^{G242D/G242D}$ double-mutant embryos (M, N). (O) Statistic result for E-N. Error bars represent ± s.e.m of 15-30 embryos. p values are denoted by asterisks; (**)P<0.01; (***)P<0.001 (ANOVA followed by LSD post hoc test for multiple comparisons).

Figure 5. **DNA binding property is indispensable for Irf2bp2b in regulating NMP cell fate choice.** (A-L) *Irf2bp2b* mRNA rescue assays in *irf2bp2b*$^{-/-}$ embryos. (A) Structure of variant forms of Irf2bp2b, including WT, ZM, tet-ZM, and RM mutant. (B-L) *Mpx* and *mfap4* probes were used in WISH to examine rescue effect with *irf2bp2b* ZM (F, G), tet-ZM (H, I), and RM mutant mRNA injections (J, K). (L) Error bars represent ± s.e.m of 15-30 embryos. p values are denoted by asterisks; (ns): no statistical significance; (**)P<0.01; (***)P<0.001(ANOVA followed by LSD post hoc test for multiple comparisons).

Figure 6. **DNA binding property is indispensable for Irf2bp2b in regulating NMP cell fate choice (continued).** (A) Ability of Irf2bp2b mutants to repress the zebrafish *pu.1* promoter (-1.7kb). Error bars represent ± s.e.m of at least 3 replicates. p values are denoted by asterisks; (***)P<0.001 (ANOVA followed by LSD post hoc test for multiple comparisons). (B) Irf2bp2b represses luciferase expression from the *pu.1* promoter 132bp A region (from -1308bp to -1439bp). Error bars represent ± SD of at least 3 replicates. p values are denoted by asterisks; (***)P<0.001 (Student's t test). (C) CHIP-PCR analysis of *pu.1* promoter A region in zebrafish embryos expressing GFP, Irf2bp2b-GFP or Irf2bp2b$^{R55/59L}$-GFP using an anti-GFP antibody. The position of the primers used to amplify the *pu.1* promoter A region are indicated with red arrows. Error bars represent ± s.e.m of at least 3 replicates. p values are denoted by asterisks; (****)P<0.0001 (ANOVA followed by LSD post hoc test for multiple comparisons). (D) Luciferase repression assays of Irf2bp2b mutants on zebrafish *pu.1* promoter (-1.7kb). Error bars represent ± s.e.m of at least 3 replicates. p values are denoted by asterisks; (***)P<0.001 (ANOVA followed by LSD post hoc test for multiple comparisons). (E-J) *Irf2bp2b*$^{R55/59L}$ mRNA rescue assays in *irf2bp2b*$^{-/-}$ mutant embryos. *Mpx* and *mfap4* probes were used in WISH to examine rescue effects associated with *Irf2bp2b*$^{R55/59L}$ mutant mRNA injection. (K) Error bars represent ± s.e.m of at least 3 replicates. p values are denoted by asterisks; (***)P<0.001 (ANOVA followed by LSD post hoc test for multiple comparisons).

Figure 7. **SUMOylation is indispensable for transcription repression of Irf2bp2b.** (A) Western blot analysis (anti-HA) of HA-tagged WT and Irf2bp2b^{K496R} mutant proteins

expressed in HEK293T cells. (B) Structure of variant forms of Irf2bp2b, including WT, Irf2bp2b^{K496R}, and Irf2bp2b-SUMO mutant. (C) Western blot analysis (anti-HA) of HA-tagged WT, Irf2bp2b^{K496R} and Irf2bp2b^{E498A} mutant proteins expressed in HEK293T cells. (D) HA tagged WT or Irf2bp2b^{K496R} mutant protein was immunoprecipitated (IP) with an anti-HA antibody from HEK293T cells co-expressing GFP-SUMO, and SUMOylated Irf2bp2b protein was detected by western blot with an anti-GFP antibody. (E) Repression of luciferase expression from the zebrafish *pu.1* promoter (-1.7kb) by Irf2bp2b mutants. Error bars represent ± s.e.m of at least 3 replicates. p values are denoted by asterisks; (***)P<0.001 (ANOVA followed by LSD post hoc test for multiple comparisons). (F-M) *Irf2bp2b*-SUMO and *irf2bp2b*^{K496R} rescue assays in *irf2bp2b*$^{-/-}$ mutant embryos. *Mpx* and *mfap4* probes were used in WISH to examine rescue effects performed with *irf2bp2b*^{K496R} mutant (J, K), and *irf2bp2b-sumo* (L, M) mRNA injections. (N) Error bars represent ± s.e.m of 15-30 embryos. p values are denoted by asterisks; (ns): no statistical significance; (**)P<0.01; (***)P<0.001 (ANOVA followed by LSD post hoc test for multiple comparisons).

Figure 8. Irf2bp2b mediates the antagonistic effect of C/ebpα on *pu.1*. (A) Schematic diagram of zebrafish *irf2bp2b* promoter (-2.2kb) (top panel). C/ebpα activation on *irf2bp2b* promoter was measured by luciferase activity assay (bottom panel). Error bars represent ± SD of at least 3 replicates. p values are denoted by asterisks; (****)P<0.0001 (Student's t test). (B, C) Representative fluorescent images of transient mCherry expression at 20hpf of WT and *c/ebpα* overexpressing embryos injected with an *irf2bp2b*:mCherry construct, respectively (bottom panel). Corresponding bright field images (top panel). (D) Schematic diagram of zebrafish *irf2bp2b* promoter (-2.2kb), in which two putative C/ebpα binding sites are predicted (CS1, CS2) (top panel). Luciferase activity assays of C/ebpα activation on the *irf2bp2b* CS1 and CS2 mutant promoters (bottom panel). Data shown are the means ± SD of at least three independent experiments. Error bars represent ± SD of at least 3 replicates. p values are denoted by asterisks; (***)P<0.001 (Student's t test). (E-L) *C/ebpα* mRNA overexpression in WT and *irf2bp2b*$^{-/-}$ mutant embryos. *Mpx* and *mfap4* probes were used in WISH to examine rescue effect. (M) Statistical results for E-L.

Error bars represent ± s.e.m of 15-30 embryos. p values are denoted by asterisks; (ns): no

statistical significance; (*)P<0.1; (**)P<0.01; (***)P<0.001 (ANOVA followed by LSD post hoc test for multiple comparisons). (N) Schematic depiction of neutrophil and macrophage fate regulation in WT (left panel) and *irf2bp2b*$^{-/-}$ (right panel) zebrafish.

Figure 1

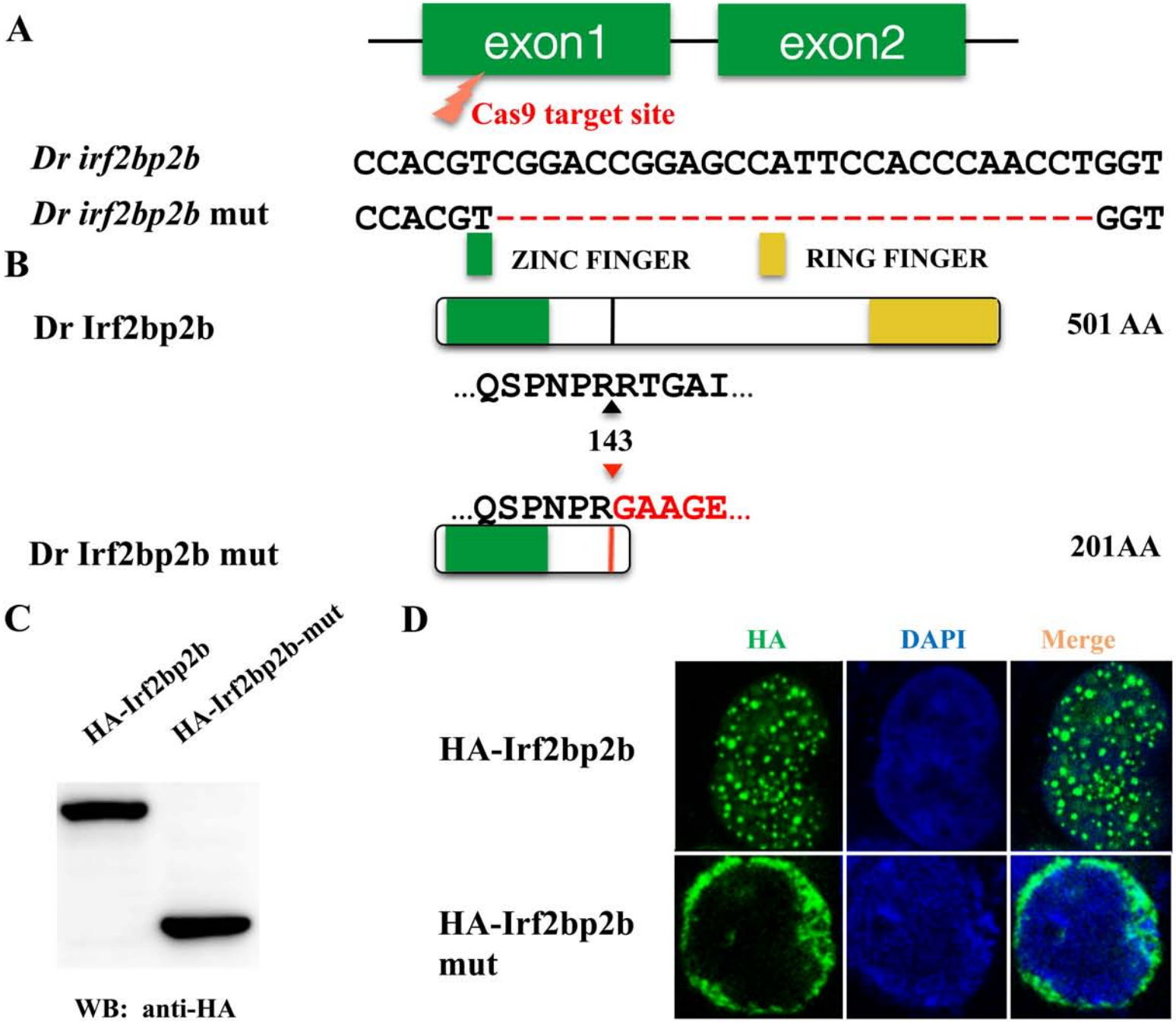
A
exon1
exon2
Cas9 target site
Dr irf2bp2b
CCACGTCGGACCGGAGCCATTCCACCCAACCTGGT
Dr irf2bp2b mut
CCACGT----------GGT
B
ZINC FINGER
RING FINGER
Dr Irf2bp2b
501 AA
...QSPNPRRTGAI...
143
...QSPNPRGAAGE...
Dr Irf2bp2b mut
201AA
C
HA-Irf2bp2b
HA-Irf2bp2b-mut
WB: anti-HA
D
HA
DAPI
Merge
HA-Irf2bp2b
HA-Irf2bp2b mut

Figure 2

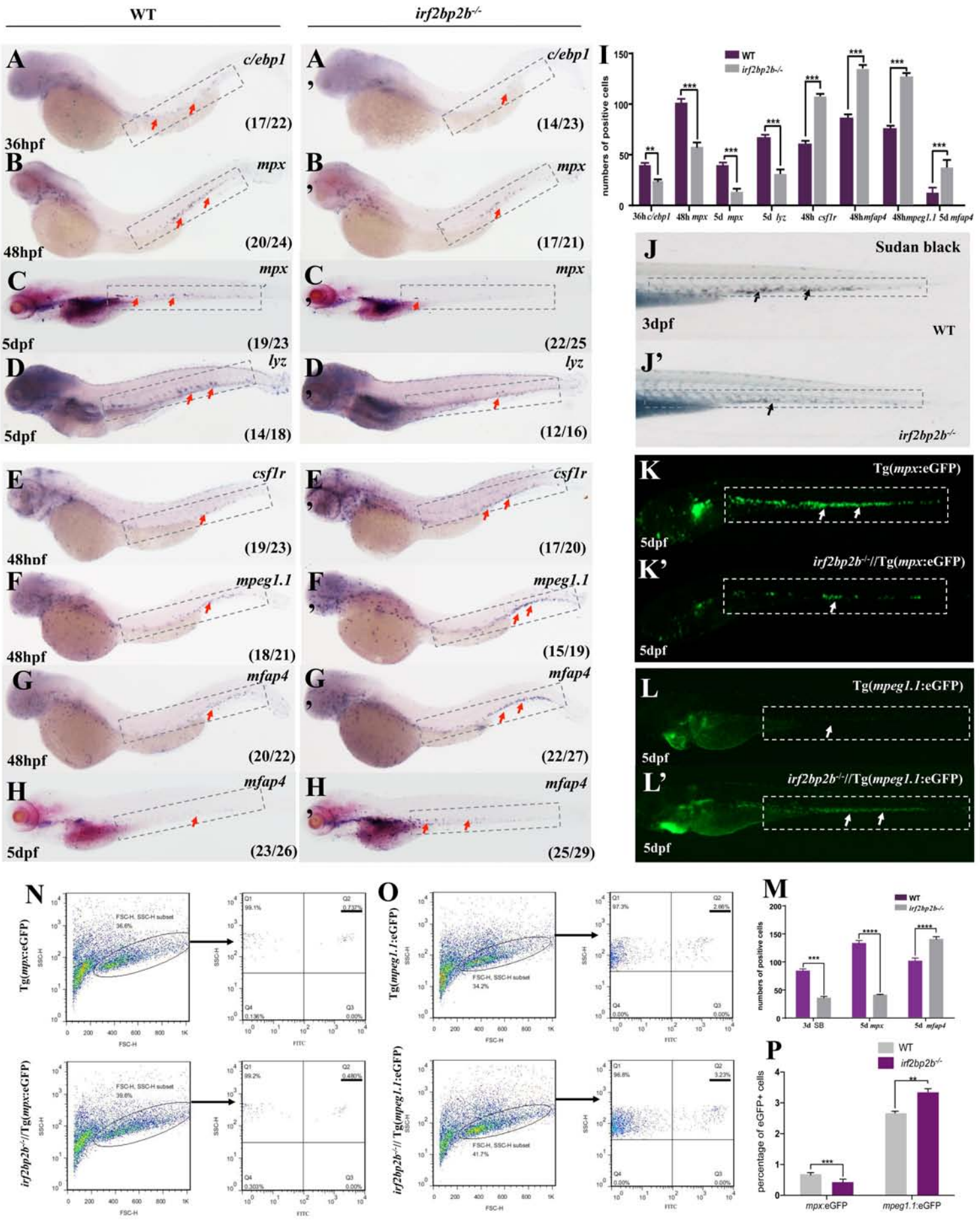
WT
irf2bp2b-/-
A
c/ebp1
(17/22)
36hpf
A'
(14/23)
B
mpx
(20/24)
48hpf
B'
(17/21)
C
mpx
(19/23
5dpf
C'
(22/25
D
lyz
(14/18)
5dpf
D'
(12/16)
E
csf1r
(19/23)
48hpf
E'
(17/20)
F
mpeg1.1
(18/21)
48hpf
F'
(15/19)
G
mfap4
(20/22)
48hpf
G'
(22/27)
H
mfap4
(23/26)
5dpf
H'
(25/29)
I
WT
irf2bp2b-/-
numbers of positive cells
36h c/ebp1
48h mpx
5d mpx
5d lyz
48h csf1r
48h mfap4
48h mpeg1.1
5d mfap4
J
Sudan black
3dpf
WT
J'
irf2bp2b-/-
K
Tg(mpx:eGFP)
5dpf
K'
irf2bp2b-/-/Tg(mpx:eGFP)
5dpf
L
Tg(mpeg1.1:eGFP)
5dpf
L'
irf2bp2b-/-/Tg(mpeg1.1:eGFP)
5dpf
N
Tg(mpx:eGFP)
irf2bp2b-/-/Tg(mpx:eGFP)
FSC-H, SSC-H subset
36.6%
39.6%
FSC-H
SSC-H
FITC
Q1
Q2
Q3
Q4
99.1%
0.737%
0.136%
0.00%
89.2%
0.480%
0.303%
0.00%
O
Tg(mpeg1.1:eGFP)
irf2bp2b-/-/ Tg(mpeg1.1:eGFP)
34.2%
41.7%
97.3%
2.06%
0.00%
0.00%
96.8%
3.23%
0.00%
0.00%
M
WT
irf2bp2b-/-
numbers of positive cells
3d SB
5d mpx
5d mfap4
P
WT
irf2bp2b-/-
percentage of eGFP+ cells
mpx:eGFP
mpeg1.1:eGFP

Figure 3

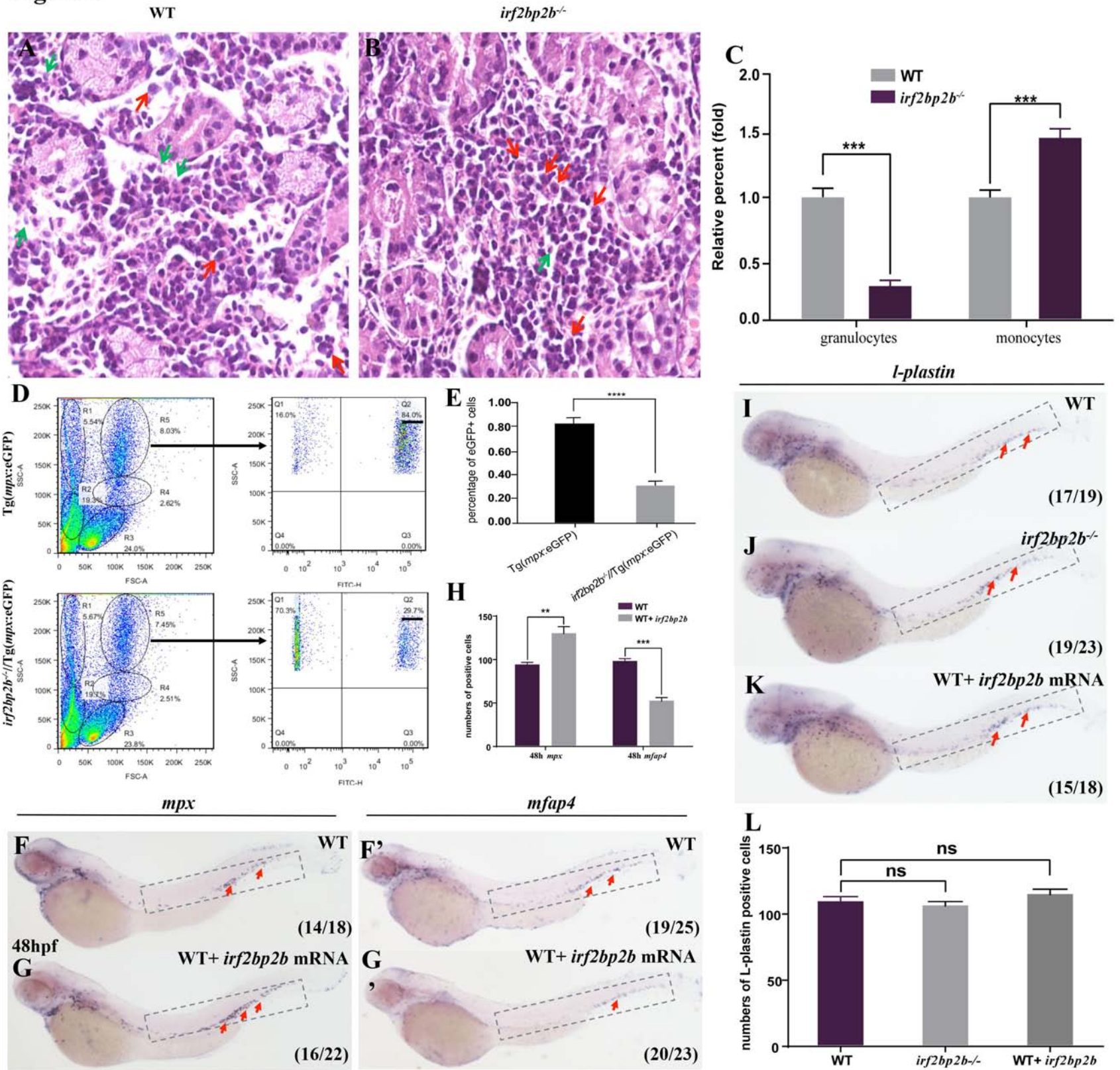
WT
irf2bp2b-/-
A
B
C
WT
irf2bp2b-/-
Relative percent (fold)
2.0
1.5
1.0
0.5
0.0
***
***
granulocytes
monocytes
D
Tg(mpx:eGFP)
irf2bp2b-/-//Tg(mpx:eGFP)
SSC-A
FSC-A
FITC-H
R1
R2
R3
R4
R5
Q1
Q2
Q3
Q4
E
percentage of eGFP+ cells
****
Tg(mpx:eGFP)
irf2bp2b-/-//Tg(mpx:eGFP)
H
numbers of positive cells
WT
WT+ irf2bp2b
**
***
48h mpx
48h mfap4
l-plastin
I
WT
(17/19)
J
irf2bp2b-/-
(19/23)
K
WT+ irf2bp2b mRNA
(15/18)
mpx
mfap4
F
WT
(14/18)
48hpf
G
WT+ irf2bp2b mRNA
(16/22)
F'
WT
(19/25)
G'
WT+ irf2bp2b mRNA
(20/23)
L
numbers of L-plastin positive cells
ns
ns
WT
irf2bp2b-/-
WT+ irf2bp2b

Figure 4

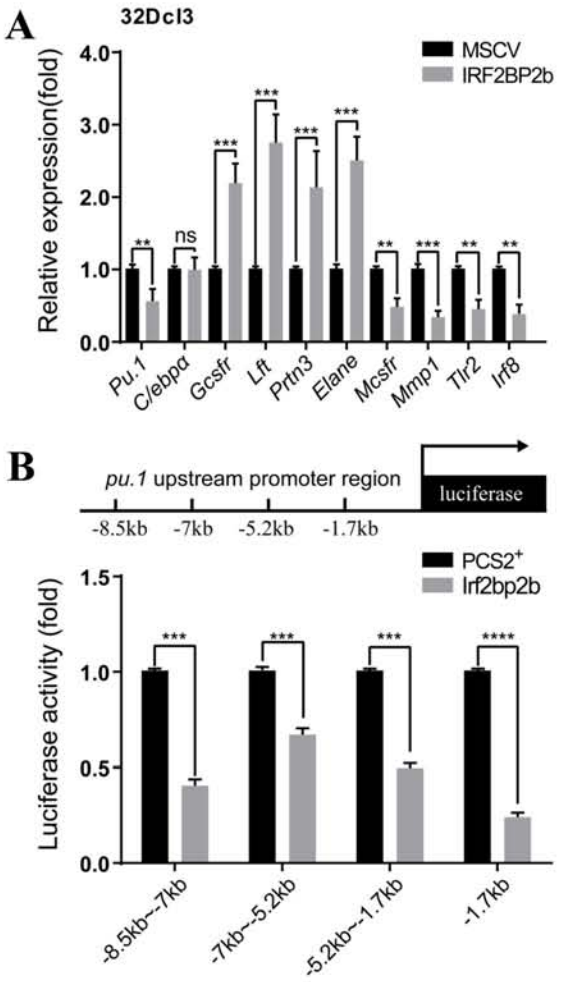
A
32Dcl3
MSCV
IRF2BP2b
Relative expression(fold)
4.0
3.0
2.0
1.0
0.0
**
ns
***
***
***
**
***
**
**
Pu.1
C/ebpα
Gcsfr
Lft
Prtn3
Elane
Mcsfr
Mmp1
Tlr2
Irf8
B
pu.1 upstream promoter region
luciferase
-8.5kb
-7kb
-5.2kb
-1.7kb
PCS2+
Irf2bp2b
Luciferase activity (fold)
1.5
1.0
0.5
0.0
***
***
***
****
-8.5kb~-7kb
-7kb~-5.2kb
-5.2kb~-1.7kb
-1.7kb

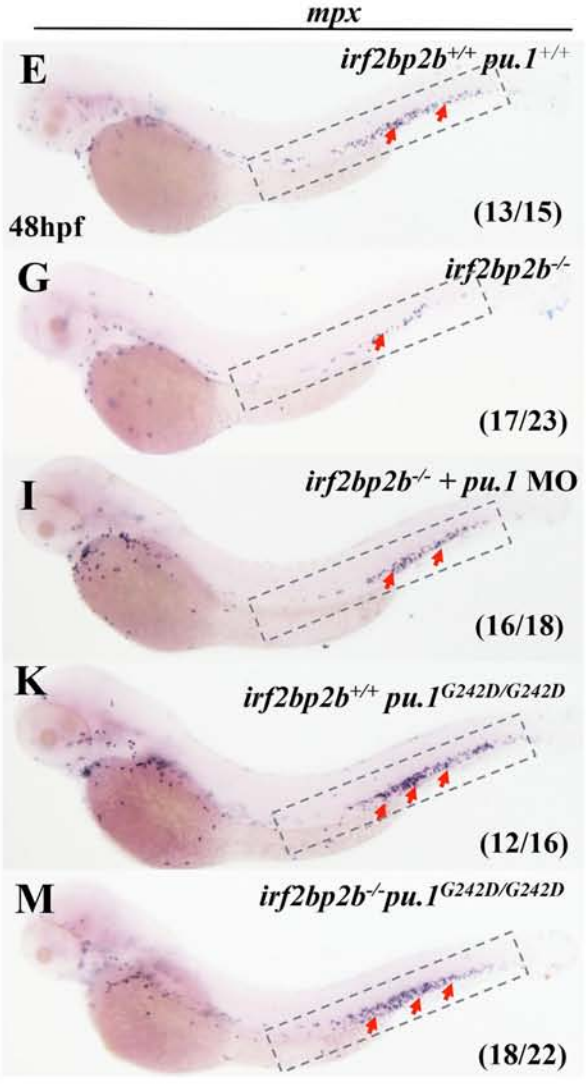
mpx
E
irf2bp2b+/+ pu.1+/+
48hpf
(13/15)
G
irf2bp2b-/-
(17/23)
I
irf2bp2b-/- + pu.1 MO
(16/18)
K
irf2bp2b+/+ pu.1G242D/G242D
(12/16)
M
irf2bp2b-/-pu.1G242D/G242D
(18/22)

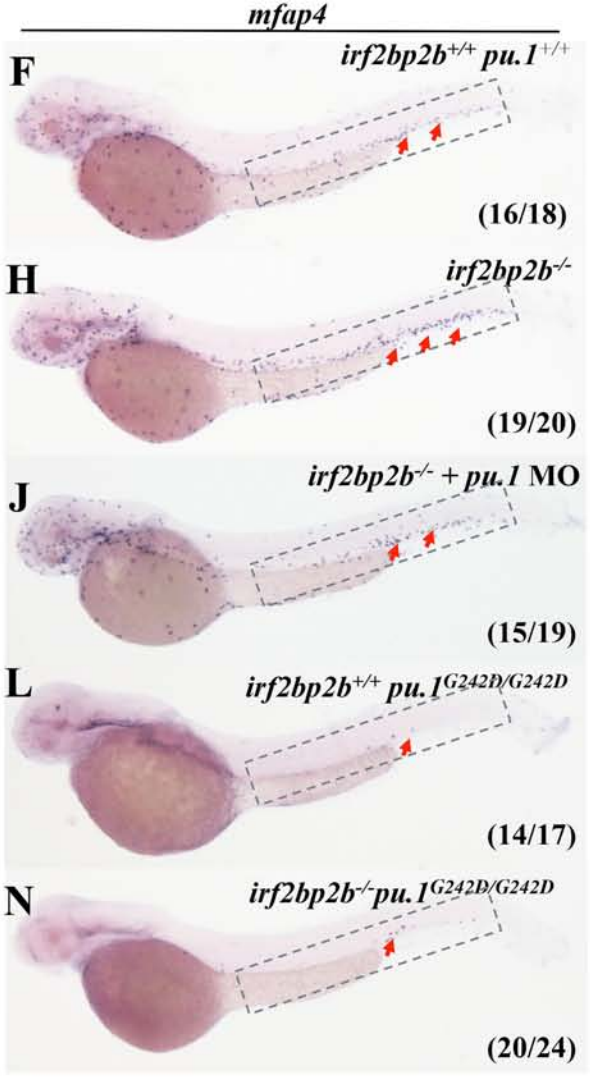
mfap4
F
irf2bp2b+/+ pu.1+/+
(16/18)
H
irf2bp2b-/-
(19/20)
J
irf2bp2b-/- + pu.1 MO
(15/19)
L
irf2bp2b+/+ pu.1G242D/G242D
(14/17)
N
irf2bp2b-/-pu.1G242D/G242D
(20/24)

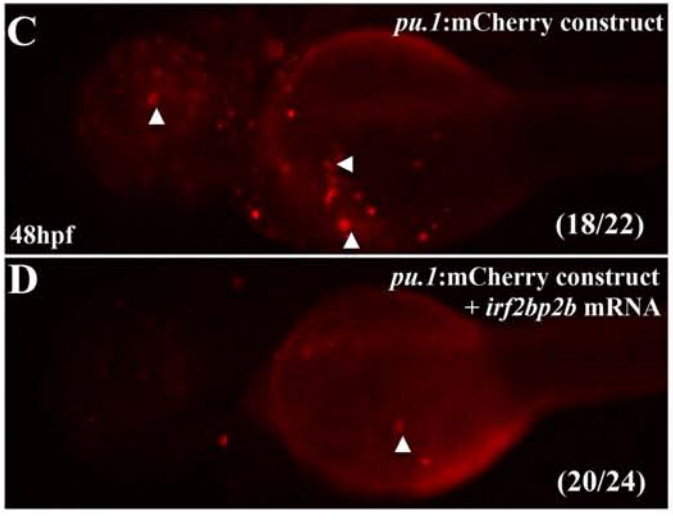
C
pu.1:mCherry construct
48hpf
(18/22)
D
pu.1:mCherry construct
+ irf2bp2b mRNA
(20/24)

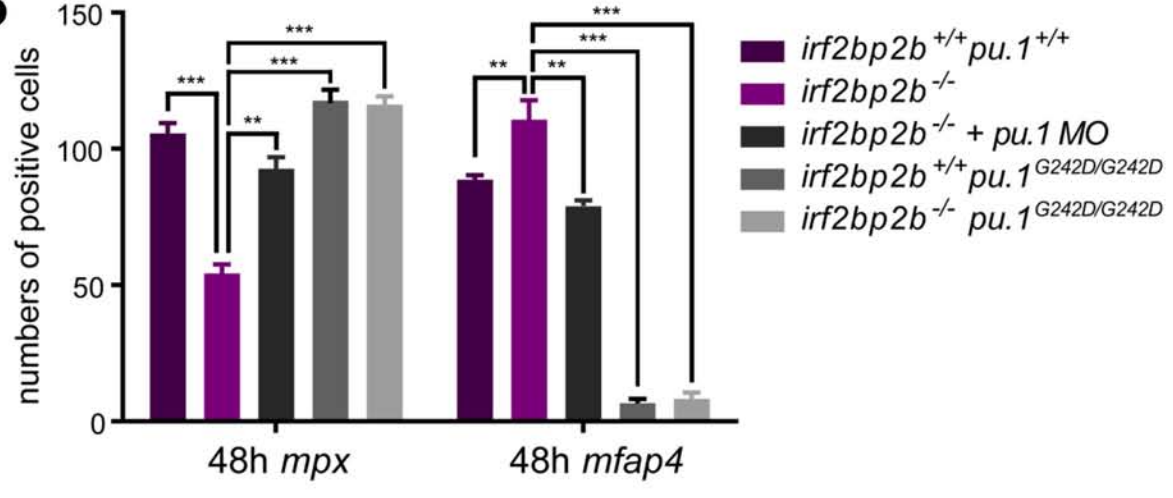
O
numbers of positive cells
150
100
50
0
***
***
***
**
**
**
***
***
48h mpx
48h mfap4
irf2bp2b +/+pu.1 +/+
irf2bp2b -/-
irf2bp2b -/- + pu.1 MO
irf2bp2b +/+pu.1 G242D/G242D
irf2bp2b -/- pu.1 G242D/G242D

Figure 5

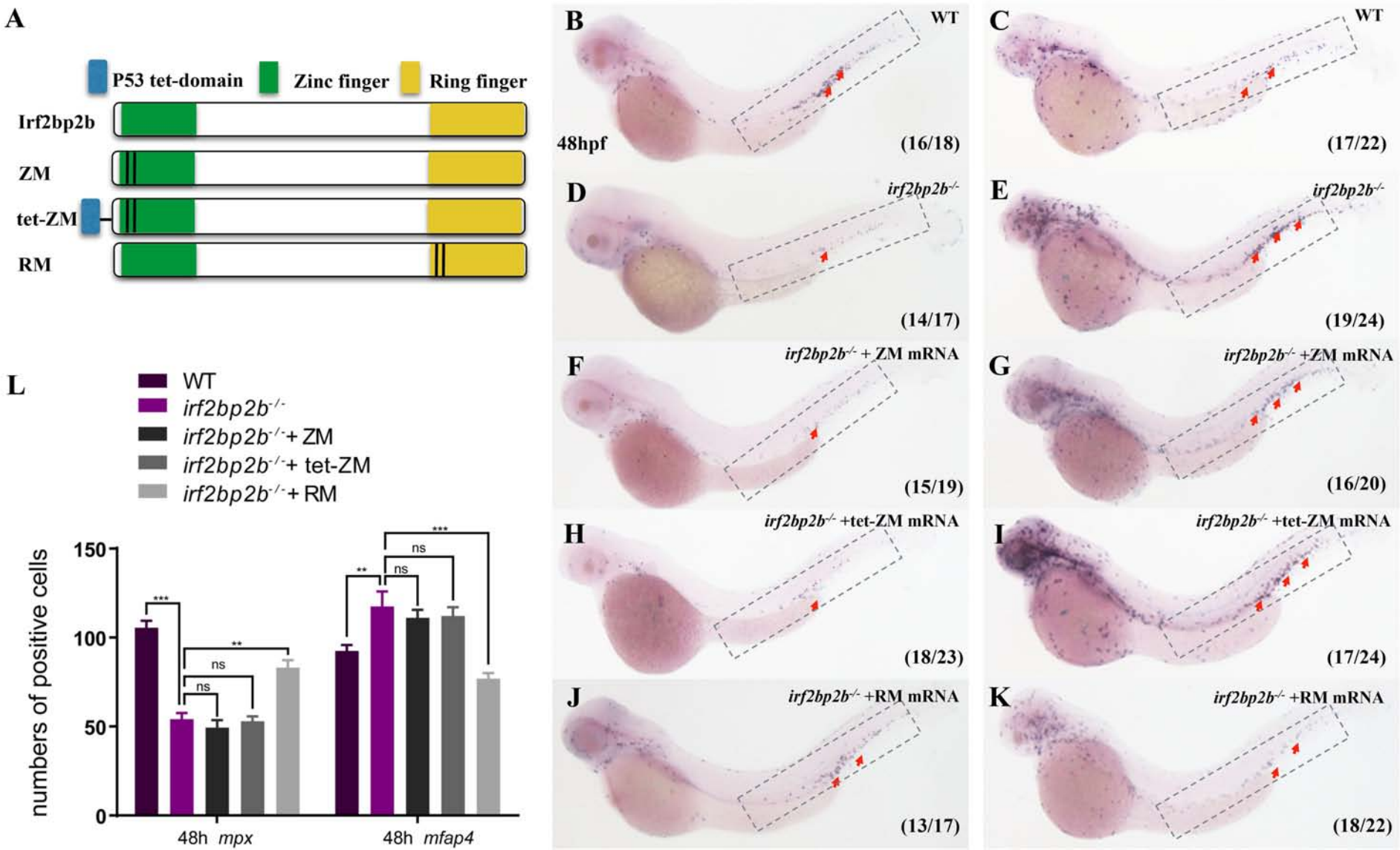
A
P53 tet-domain
Zinc finger
Ring finger
Irf2bp2b
ZM
tet-ZM
RM
mpx
mfap4
B
WT
48hpf
(16/18)
C
WT
(17/22)
D
irf2bp2b-/-
(14/17)
E
irf2bp2b-/-
(19/24)
F
irf2bp2b-/- + ZM mRNA
(15/19)
G
irf2bp2b-/- +ZM mRNA
(16/20)
H
irf2bp2b-/- +tet-ZM mRNA
(18/23)
I
irf2bp2b-/- +tet-ZM mRNA
(17/24)
J
irf2bp2b-/- +RM mRNA
(13/17)
K
irf2bp2b-/- +RM mRNA
(18/22)
L
WT
irf2bp2b-/-
irf2bp2b-/-+ ZM
irf2bp2b-/-+ tet-ZM
irf2bp2b-/-+ RM
numbers of positive cells
150
100
50
0
***
**
ns
ns
**
ns
***
48h mpx
48h mfap4

Figure 6

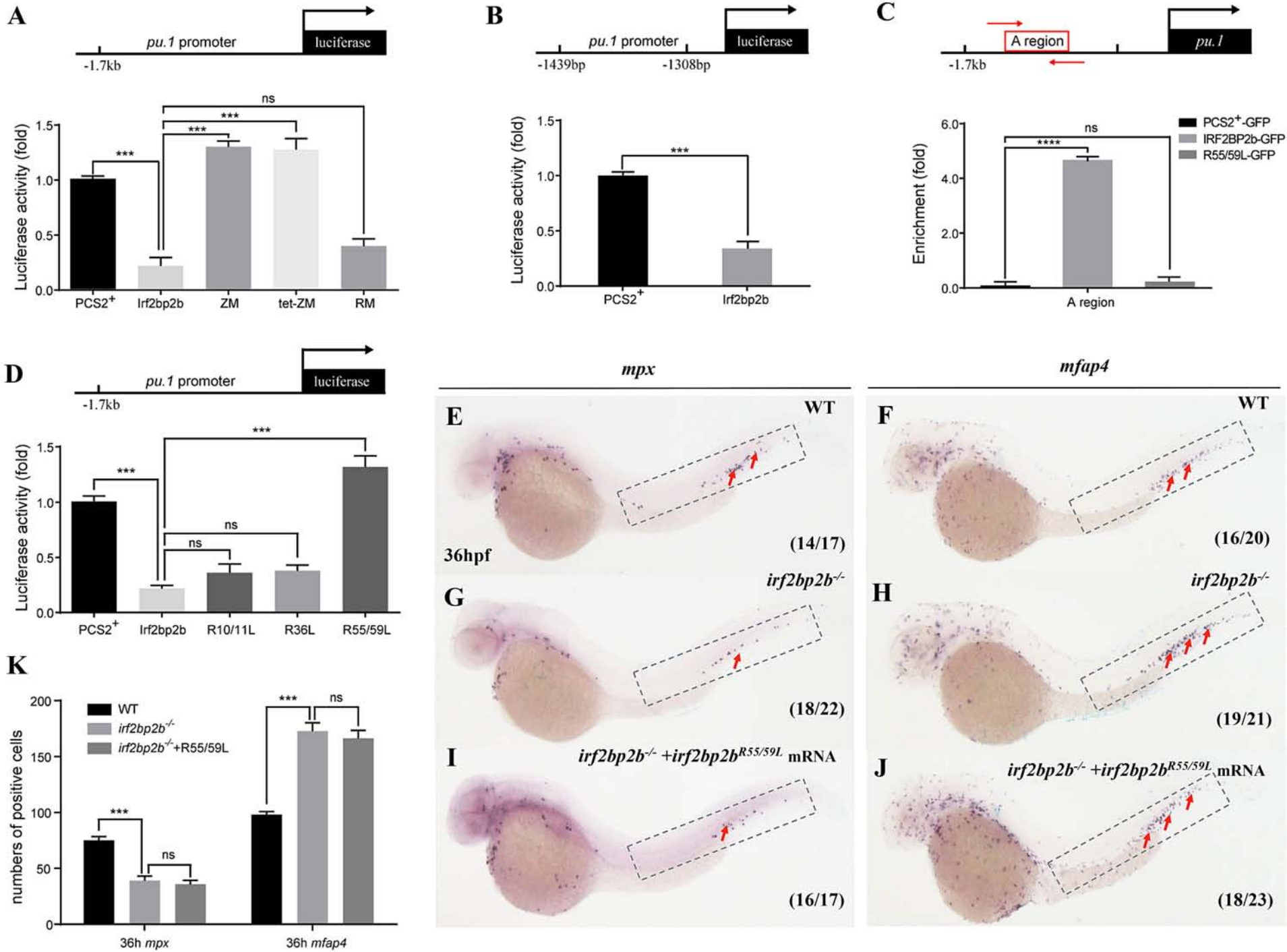
A
pu.1 promoter
luciferase
-1.7kb
Luciferase activity (fold)
PCS2+
Irf2bp2b
ZM
tet-ZM
RM
B
pu.1 promoter
luciferase
-1439bp
-1308bp
Luciferase activity (fold)
PCS2+
Irf2bp2b
C
A region
pu.1
-1.7kb
Enrichment (fold)
PCS2+-GFP
IRF2BP2b-GFP
R55/59L-GFP
A region
D
pu.1 promoter
luciferase
-1.7kb
Luciferase activity (fold)
PCS2+
Irf2bp2b
R10/11L
R36L
R55/59L
mpx
mfap4
E
WT
36hpf
(14/17)
F
WT
(16/20)
G
irf2bp2b-/-
(18/22)
H
irf2bp2b-/-
(19/21)
I
irf2bp2b-/- +irf2bp2bR55/59L mRNA
(16/17)
J
irf2bp2b-/- +irf2bp2bR55/59L mRNA
(18/23)
K
WT
irf2bp2b-/-
irf2bp2b-/-+R55/59L
numbers of positive cells
36h mpx
36h mfap4

Figure 7

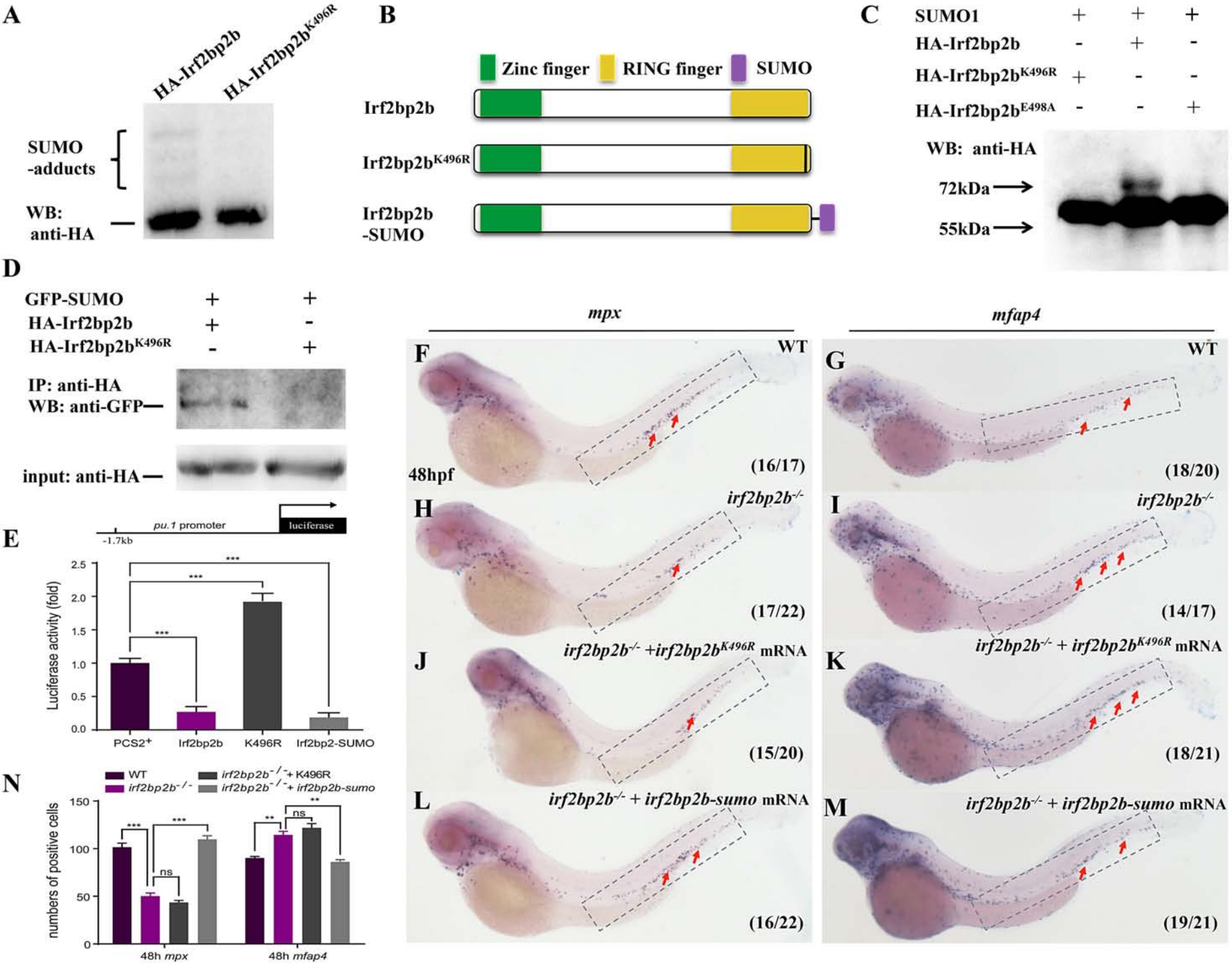
A
HA-Irf2bp2b
HA-Irf2bp2b^K496R
SUMO
-adducts
WB:
anti-HA
B
Zinc finger
RING finger
SUMO
Irf2bp2b
Irf2bp2b^K496R
Irf2bp2b
-SUMO
C
SUMO1 + + +
HA-Irf2bp2b - + -
HA-Irf2bp2b^K496R + - -
HA-Irf2bp2b^E498A - - +
WB: anti-HA
72kDa
55kDa
D
GFP-SUMO + +
HA-Irf2bp2b + -
HA-Irf2bp2b^K496R - +
IP: anti-HA
WB: anti-GFP
input: anti-HA
E
pu.1 promoter
luciferase
-1.7kb
Luciferase activity (fold)
PCS2+
Irf2bp2b
K496R
Irf2bp2-SUMO
N
WT
irf2bp2b^-/-
irf2bp2b^-/-+ K496R
irf2bp2b^-/-+ irf2bp2b-sumo
numbers of positive cells
48h mpx
48h mfap4
mpx
mfap4
F WT
48hpf
(16/17)
G WT
(18/20)
H irf2bp2b^-/-
(17/22)
I irf2bp2b^-/-
(14/17)
J irf2bp2b^-/- +irf2bp2b^K496R mRNA
(15/20)
K irf2bp2b^-/- + irf2bp2b^K496R mRNA
(18/21)
L irf2bp2b^-/- + irf2bp2b-sumo mRNA
(16/22)
M irf2bp2b^-/- + irf2bp2b-sumo mRNA
(19/21)

Figure 8

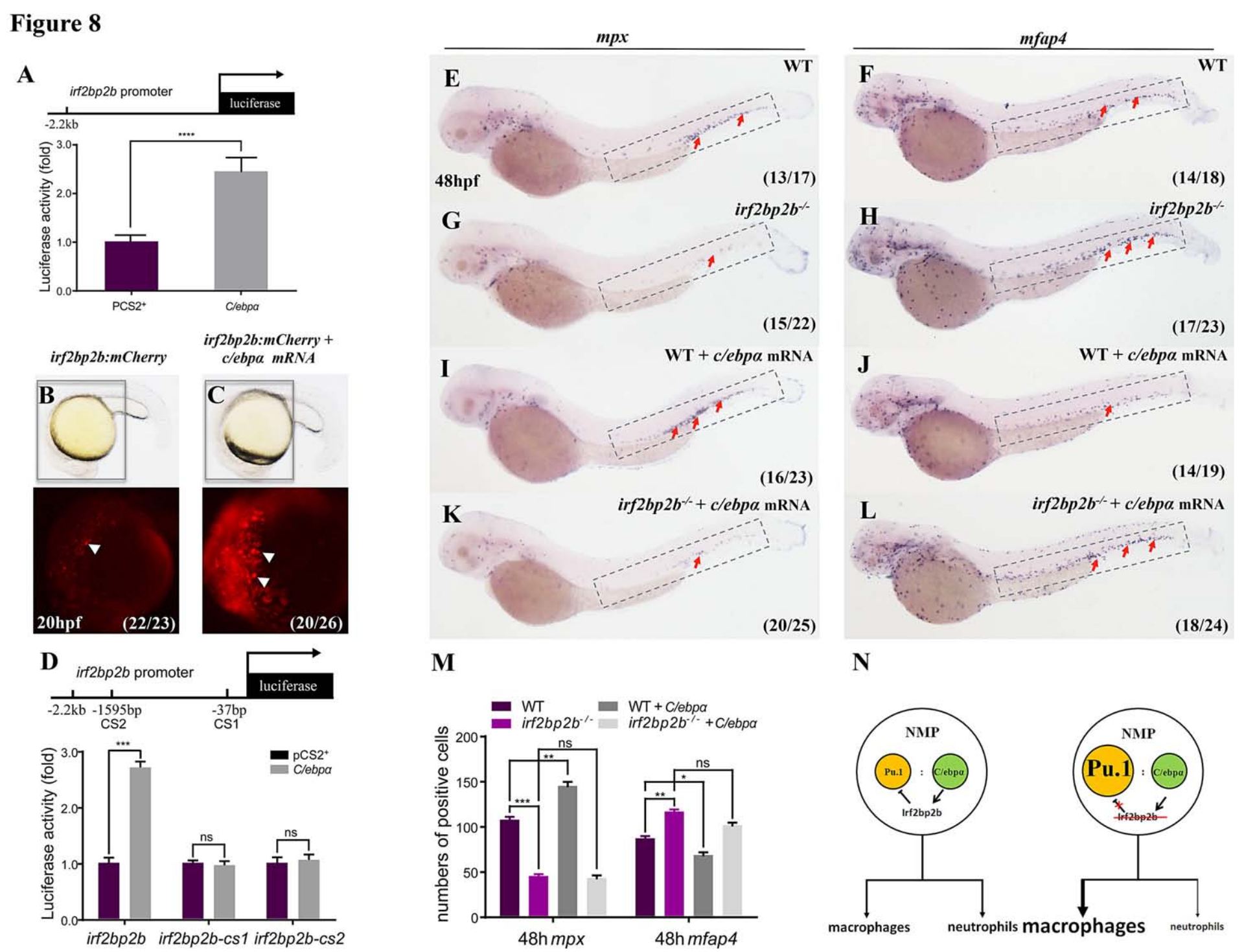
A
irf2bp2b promoter
luciferase
-2.2kb
****
Luciferase activity (fold)
3.0
2.0
1.0
0.0
PCS2+
C/ebpα
irf2bp2b:mCherry
irf2bp2b:mCherry + c/ebpα mRNA
B
C
20hpf
(22/23)
(20/26)
D
irf2bp2b promoter
luciferase
-2.2kb
-1595bp CS2
-37bp CS1
***
ns
ns
pCS2+
C/ebpα
Luciferase activity (fold)
irf2bp2b
irf2bp2b-cs1
irf2bp2b-cs2
mpx
mfap4
E
WT
48hpf
(13/17)
F
WT
(14/18)
G
irf2bp2b-/-
(15/22)
H
irf2bp2b-/-
(17/23)
I
WT + c/ebpα mRNA
(16/23)
J
WT + c/ebpα mRNA
(14/19)
K
irf2bp2b-/- + c/ebpα mRNA
(20/25)
L
irf2bp2b-/- + c/ebpα mRNA
(18/24)
M
WT
irf2bp2b-/-
WT + C/ebpα
irf2bp2b-/- +C/ebpα
numbers of positive cells
200
150
100
50
0
ns
**
***
*
48h mpx
48h mfap4
N
NMP
Pu.1
C/ebpα
Irf2bp2b
macrophages
neutrophils
NMP
Pu.1
C/ebpα
Irf2bp2b
macrophages
neutrophils

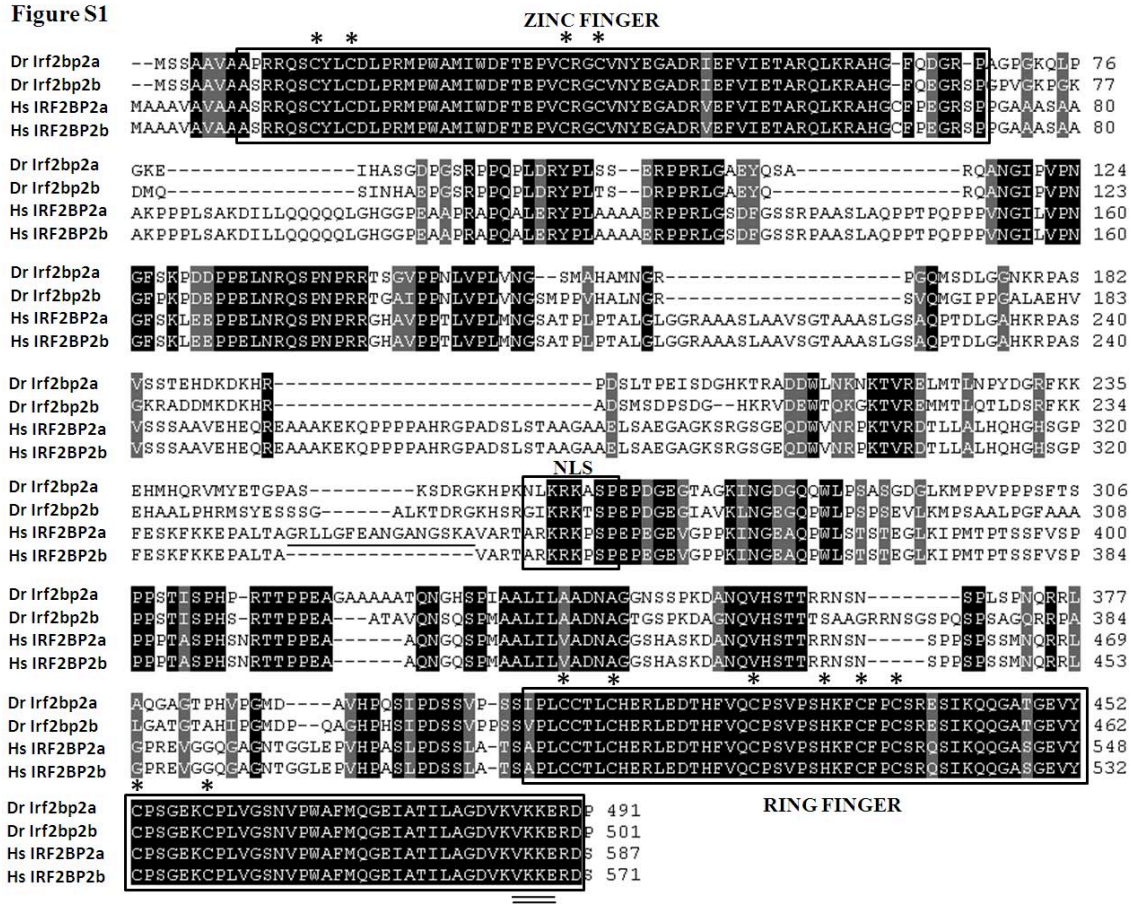

Supplemental Figure 1. Alignment of protein sequences of IRF2BP2 family members. Alignment of zebrafish (Dr) Irf2bp2a and Irf2bp2b, human (Hs) IRF2BP2a and IRF2BP2b protein sequences. Functional domains including the C4-type zinc finger and the C3HC4-type ring finger are boxed, and the critical cysteine (C) and histidine (H) residues are denoted by asterisks. The conserved nuclear localization signal (NLS) in the intermediate domain is also boxed. The extra 16 amino acids of the human IRF2BP2a isoform compared to IRF2BP2b are underlined. The consensus SUMOylation site VKKE located at the C-terminus is double underlined.

Figure S2

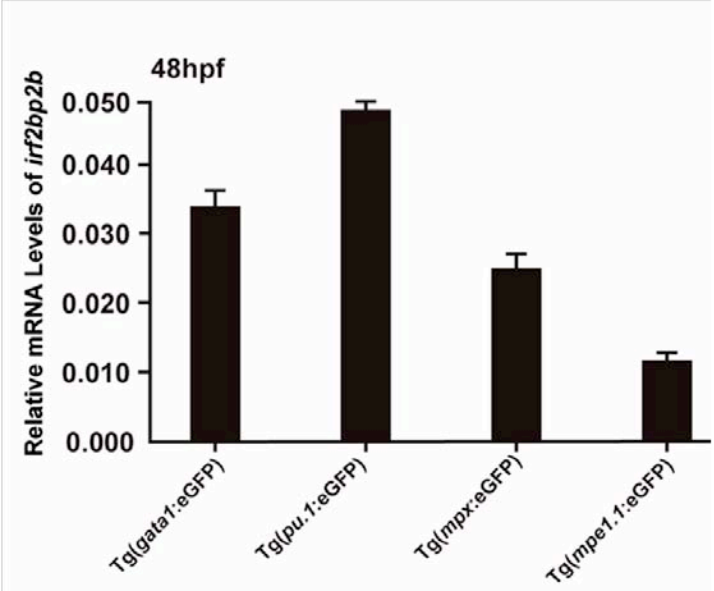

Supplemental Figure 2. Expression of *irf2bp2b* transcript in erythroid and myeloid cells. *Irf2bp2b* transcript was detected by RT-qPCR analysis in the GFP positive cells enriched from Tg(*gata1*:eGFP), Tg(*pu.1*:eGFP), Tg(*mpx*:eGFP), and Tg(*mpeg1.1*:eGFP) embryos at 48hpf, respectively. *β-actin* served as internal control.

Figure S3

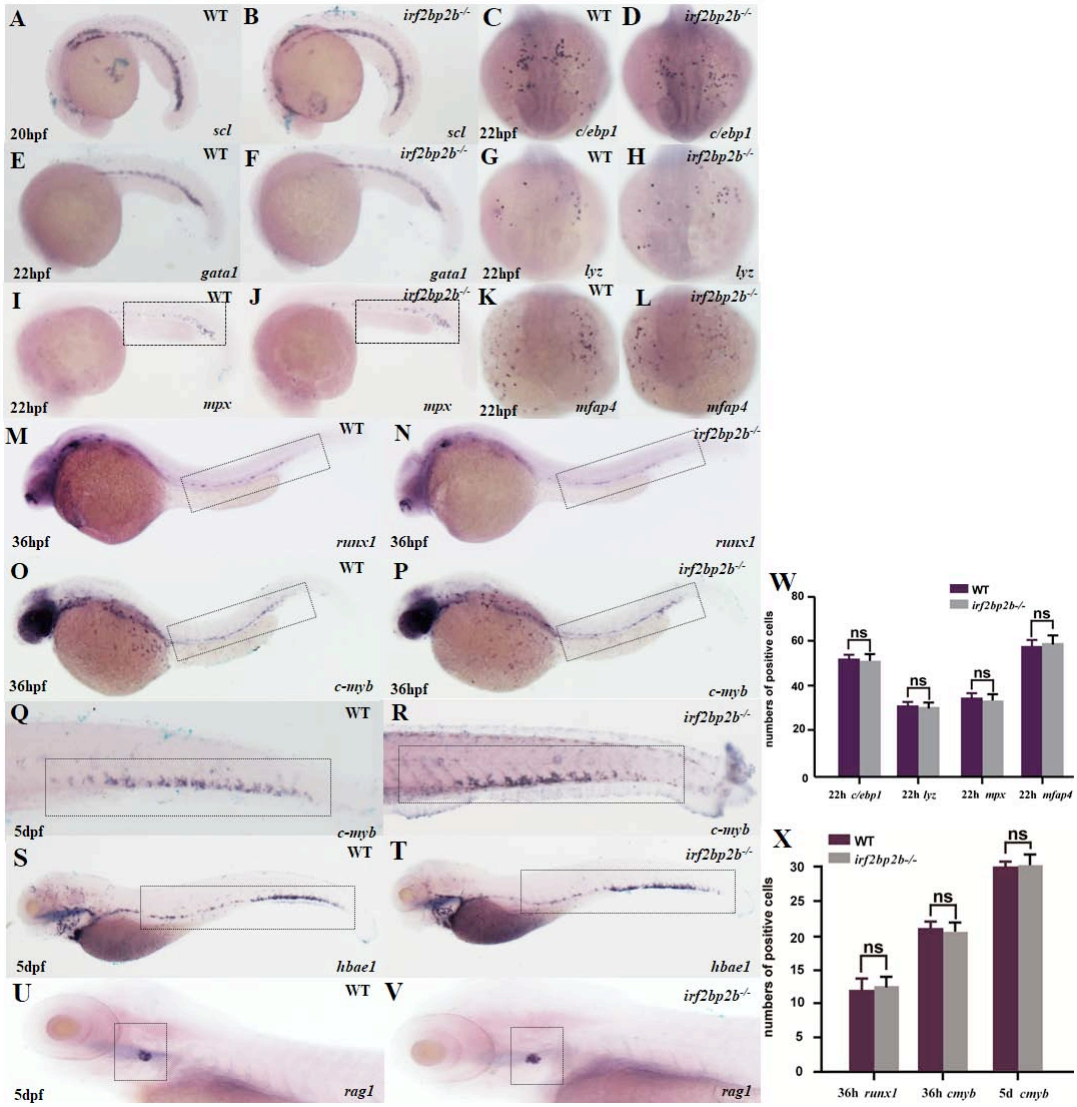

Supplemental Figure 3. Expression of lineage specific markers during primitive and definitive hematopoiesis stages in *irf2bp2b*-deficient embryos. (A-L) WISH analyses of *scl* (A, B) at 20hpf, and *c/ebp1* (C, D), *gata1* (E, F), *lyz* (G, H) *mpx* (I, J), *mfap4* (K, L) at 22hpf. (M, N) WISH analyses of *runx1* at 36hpf, (O-R) WISH analyses of *c-myb* at 36hpf and 5dpf, WISH analyses of *hbae1* (S, T), and *rag1* (U, V) at 5dpf, respectively. (W, X) Statistical results for A-L, M-R. Error bars represent ± SD of at least 15-30 embryos. p values are denoted by asterisks; (ns): no statistical significance.

Figure S4

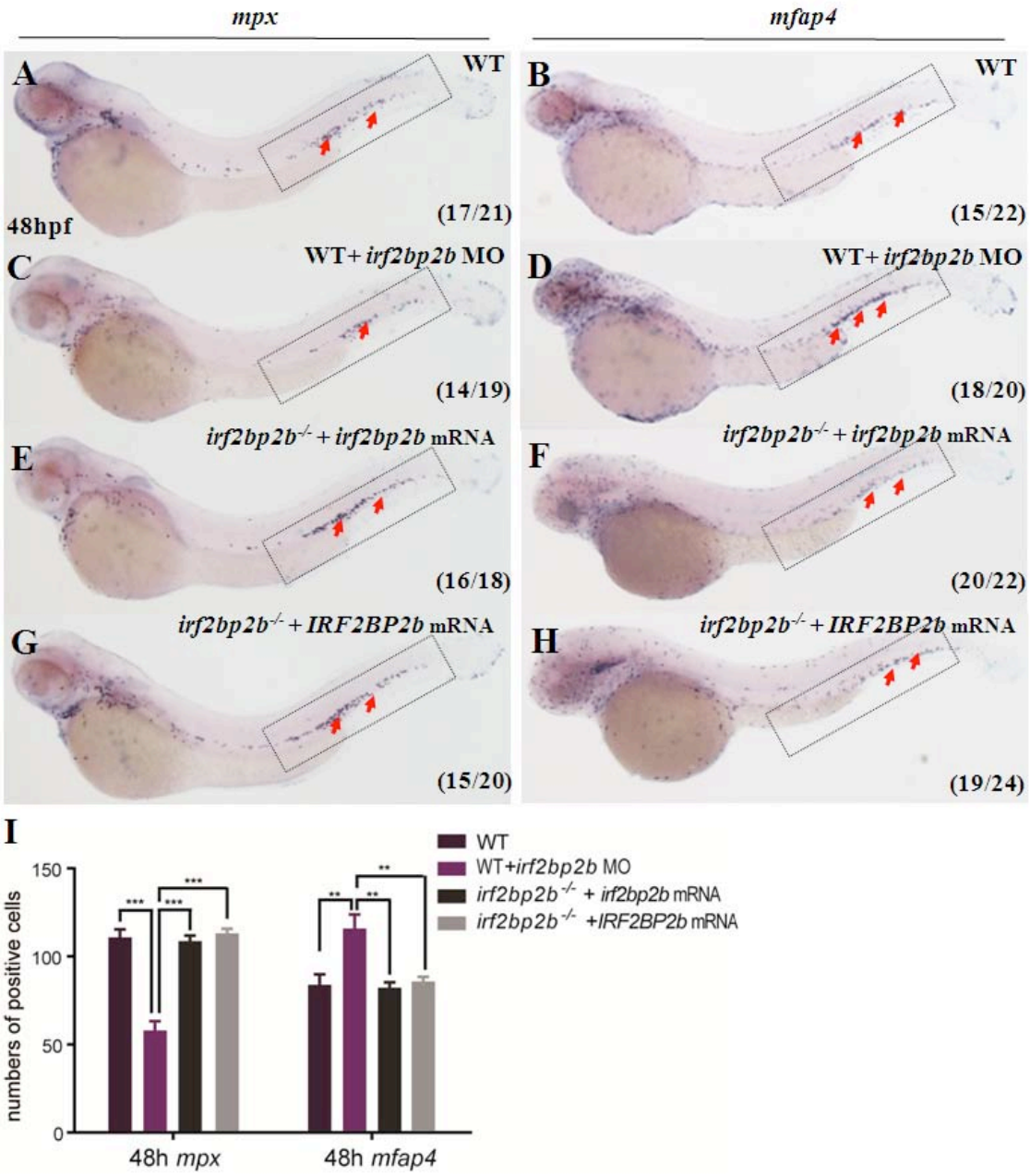

Supplemental Figure 4. **Deficiency of *irf2bp2b* leads to an expanded macrophage population at the expense of the neutrophil population during definitive myelopoiesis.** (A-D) WISH analyses of *mpx* and *mfap4* in wild type embryos injected with *irf2bp2b* gene specific MO. (E-H) Zebrafish *irf2bp2b* and human *IRF2BP2b* mRNA rescue aberrant myelopoiesis phenotype in *irf2bp2b*$^{-/-}$ mutant embryos. (I) Statistical results for A-H. Error bars represent ± s.e.m of at least 15-30 embryos. p values are denoted by asterisks; (**) P<0.01; (***) P<0.001 (ANOVA followed by LSD post hoc test).

Figure S5

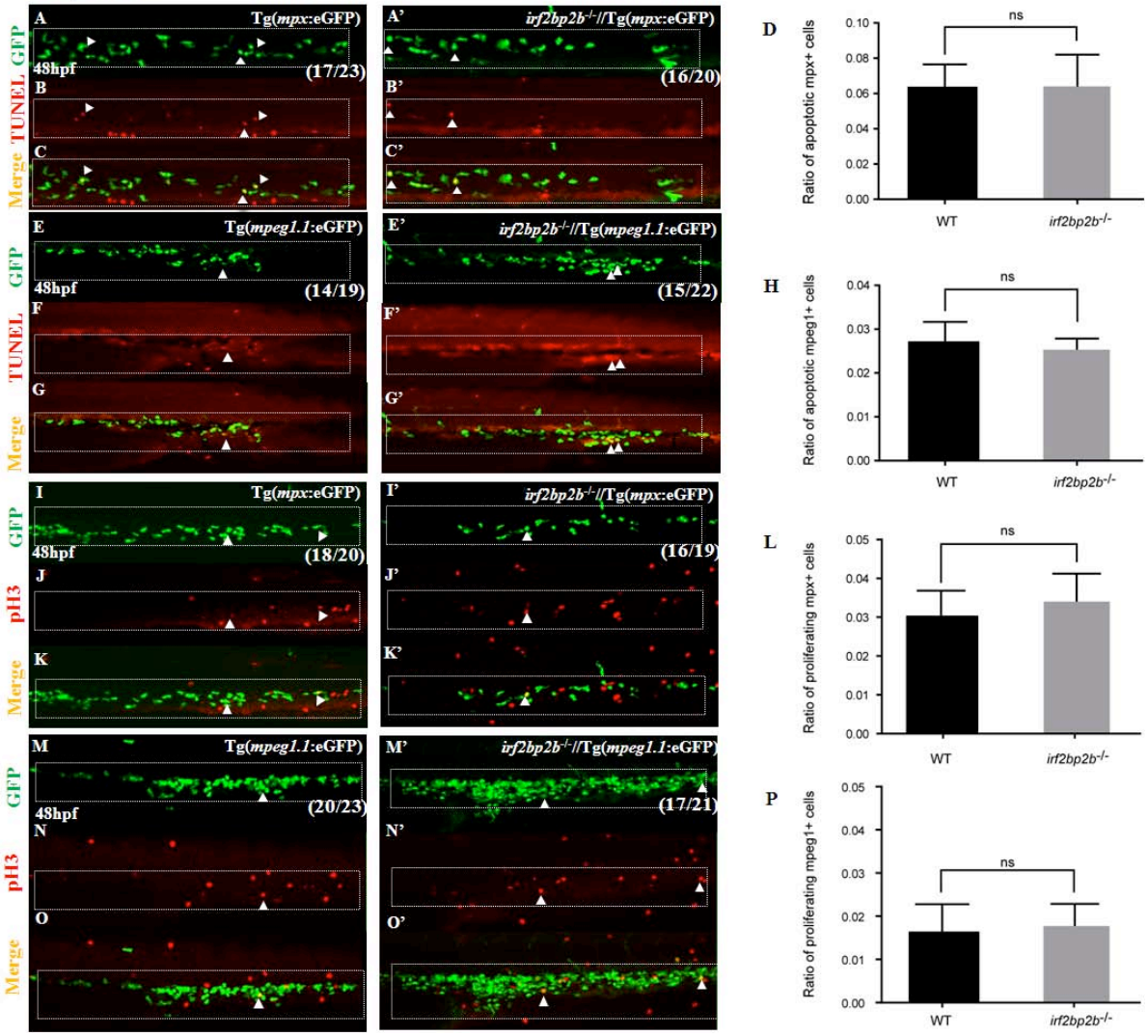

Supplemental Figure 5: **Apoptosis and proliferation of neutrophil and macrophage lineages are normal.** (A-C') Double immunostaining of GFP and TUNEL in CHT at 48hpf of Tg(*mpx*: eGFP) and *irf2bp2b*$^{-/-}$//Tg(*mpx*:eGFP) mutant embryos. (D) Statistic result for C-C'. Error bars represent ± SD of 15-30 embryos. (ns): no statistical significance. (E-G') Double immunostaining of GFP and TUNEL in CHT at 48hpf of Tg(*mpeg1.1*:eGFP) and *irf2bp2b*$^{-/-}$//Tg(*mpeg1.1*:eGFP) mutant embryos. (H) Statistic result for G-G'. Error bars represent ± SD of 15-30 embryos. (I-K') Double immunostaining of GFP and pH3 in CHT at 48hpf of Tg(*mpx*:eGFP) and *irf2bp2b*$^{-/-}$//Tg(*mpx*:eGFP) mutant embryos. (L) Statistic result for K-K'. Error bars represent ± SD of 15-30 embryos. (M-O') Double immunostaining of GFP and pH3 in CHT at 48hpf of Tg(*mpeg1.1*:eGFP) and *irf2bp2b*$^{-/-}$//Tg(*mpeg1.1*:eGFP) mutant embryos. (P) Error bars represent ± SD of 15-30 embryos.

Figure S6

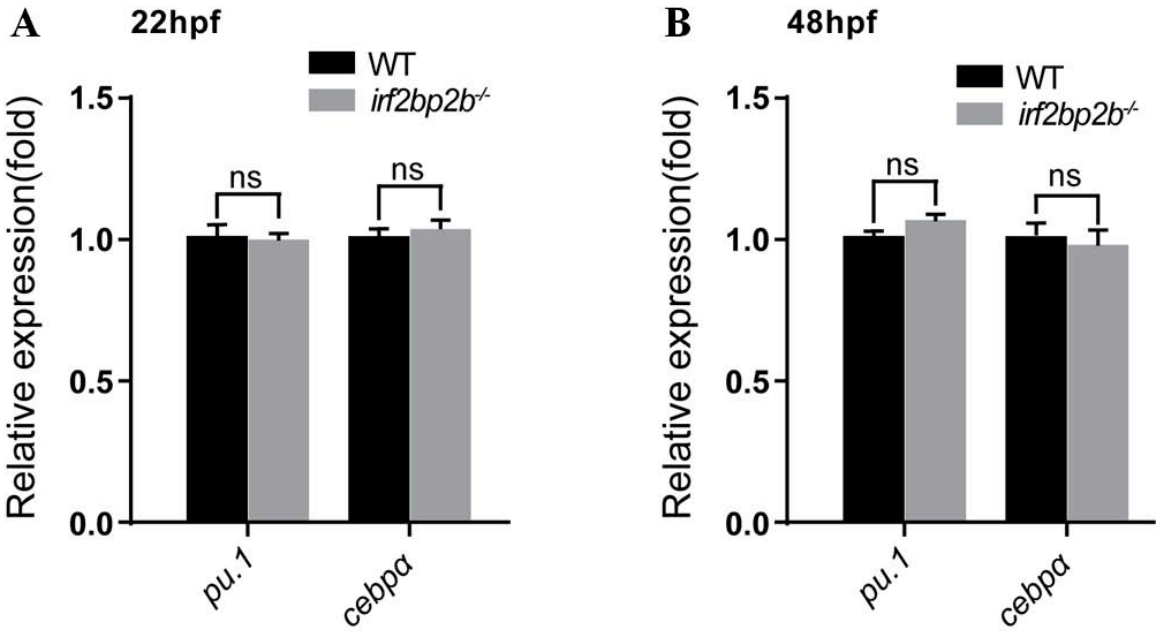

Supplemental Figure 6. **The change of *c/ebpα* and *pu.1* in NMPs might be masked.** RT-qPCR analysis of *c/ebpα* and *pu.1* in wild type and *irf2bp2b*-defecient whole embryos at 22hpf (A) and 48hpf (B). *β-actin* was used as internal control.

Figure S7

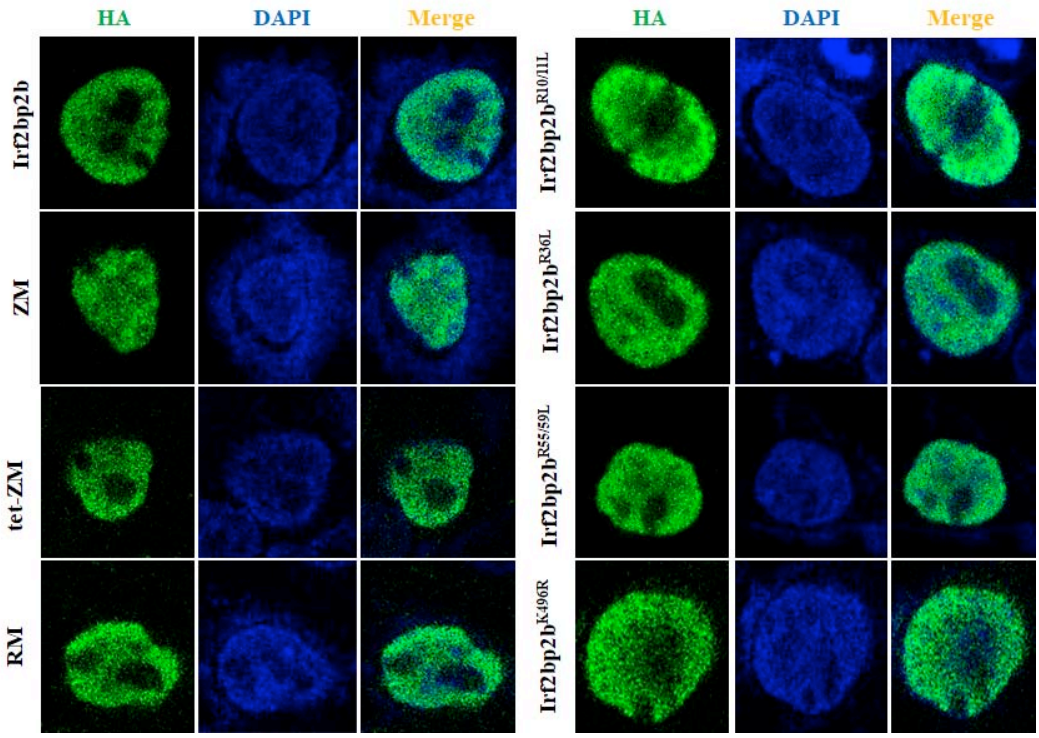

Supplemental Figure 7: Immunofluorescence analysis of HA-tagged wild type and mutant Irf2bp2b proteins. RM, ZM, tet-ZM, Irf2bp2b$^{R10/11L}$, Irf2bp2b^{R36L}, Irf2bp2b$^{R55/59L}$, and Irf2bp2b^{K496R} maintain the nuclear localization.

Figure S8

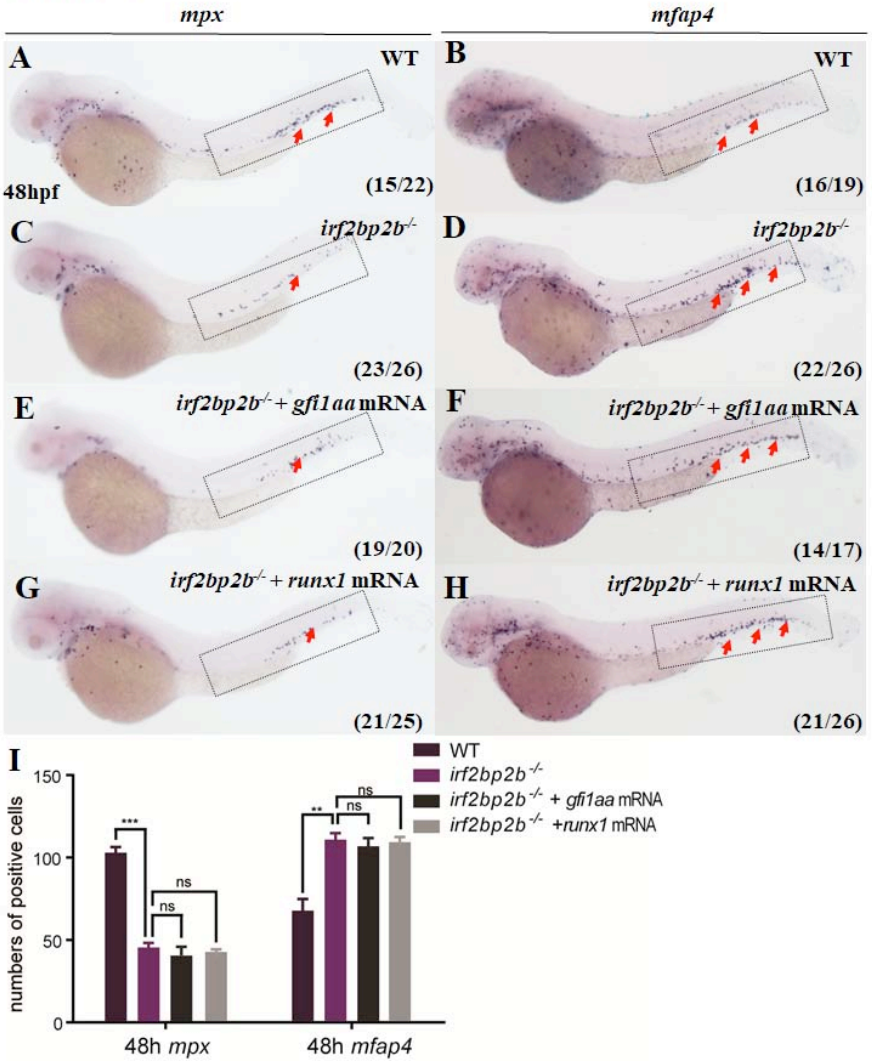

Supplemental Figure 8: *Runx1* and *gfi1aa* overexpressions in *irf2bp2b*-defecient embryos. (A-H) *Mpx* and *mfap4* were probed to monitor neutrophil and macrophage development. (I) Statistical results for A-H. Error bars represent ± s.e.m of at least 15-30 embryos. p values are denoted by asterisks; (**) P<0.01; (***) P<0.001 (ANOVA followed by LSD post hoc test).

Figure S9

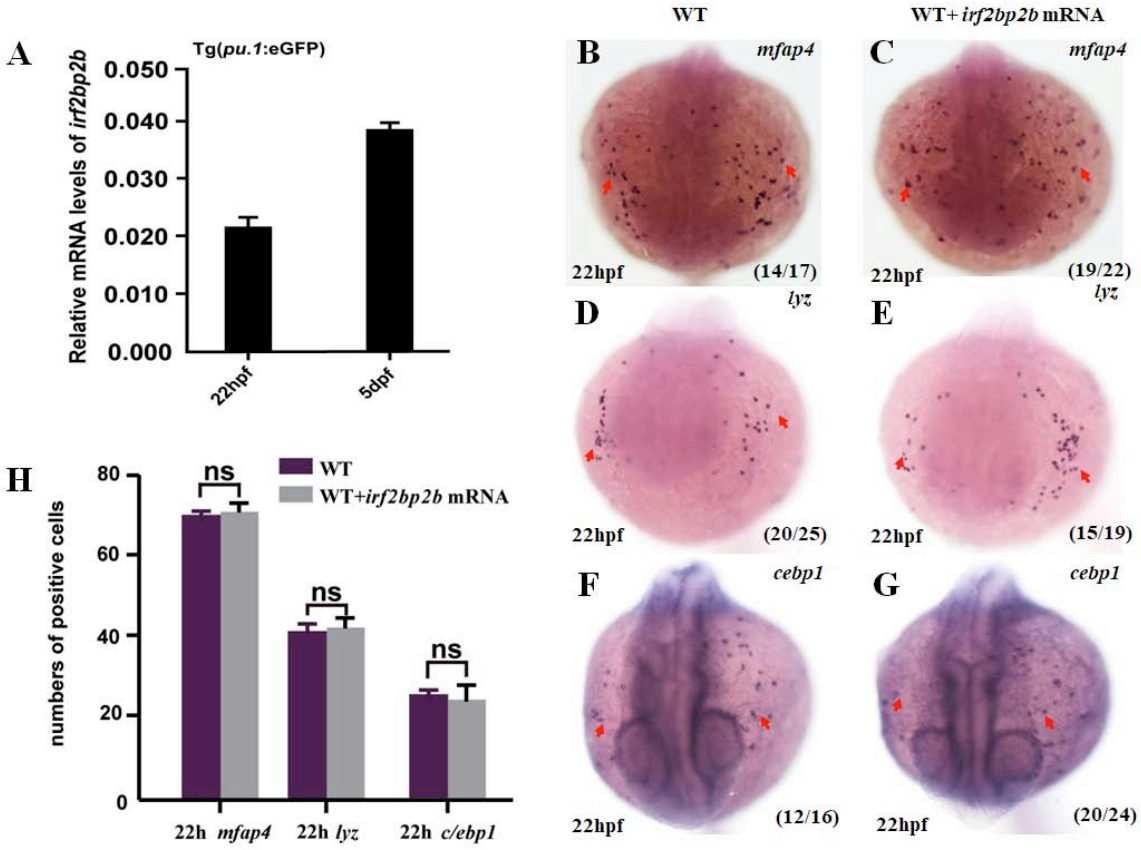

Supplemental Figure 9: *Irf2bp2b* does not play a role in RBI-originated macrophage versus neutrophil fate choice. (A) The GFP positive cells were isolated from Tg(*pu.1*:eGFP) embryos at 22hpf (primitive hematopoiesis stage) and 5dpf (definitive hematopoiesis stage), respectively. RT-qPCR analysis (*β-actin* was used as internal control) showed that *irf2bp2b* transcript was detected at both time points, suggesting that *irf2bp2b* is expressed in both primitive and definitive progenitor cells. (B-G) Overexpression of *irf2bp2b* mRNA could not impair RBI-originated myelopoiesis. (H) Statistical results for B-G. Error bars represent ± SD of at least 15-30 embryos. p values are denoted by asterisks; Error bars represent ± SD of 3 replicates. (ns): no statistical significance; (**) P<0.01; (***) P<0.001 (Student's t test).

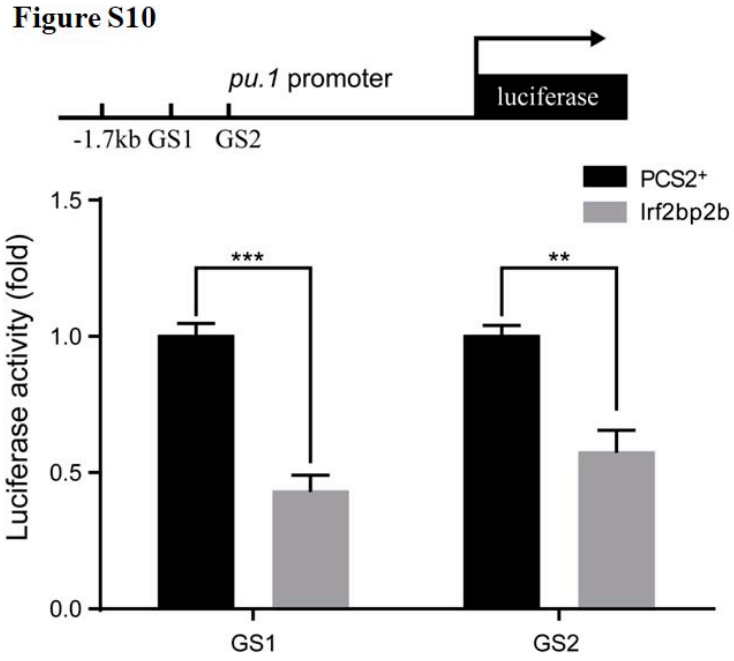

Supplemental Figure 10: Luciferase results of Irf2bp2b repression on wild type zebrafish *pu.1* promoter A region, and GS1, GS2 mutant constructs. Error bars represent ± SD of at least 3 replications. p values are denoted by asterisks; (**)P<0.01; (****)P<0.001 (Student's t test).

Supplementary Methods

Generation of *irf2bp2b* knockout line

For crisp9 mediated *irf2bp2b* knockout zebrafish generation, guide RNA (gRNA) targeting exon1 of *irf2bp2b* was designed using an online tool ZiFiT Targeter software (http://zifit.partners.org/ZiFiT), which was synthesized by cloning the annealed oligonucleotides into the sgRNA expression vector as previously described(1). The target site was 5'- GGAATGGCTCCGGTCCGACG-3'. The injected F0 founder embryos were raised to adulthood and then outcrossed with wild type zebrafish. F1 embryos carrying potential indel mutations were raised to adulthood. Then PCR amplification and sequencing were carried on genomic DNA isolated from tail clips of F1 fish to identify mutants.

Plasmid construction

Zebrafish *irf2bp2b* was cloned into $PCS2^{+}$ vector. The zebrafish *irf2bp2b* serial mutants were generated with the indicated primers (Table1). As for the luciferase reporter, the -8.5kb upstream frame of zebrafish *pu.1* was devided into four fragments and then inserted into PGL3 promoter vector (Promega) respectively. The zebrafish *irf2bp2b* gene -2.2kb upstream sequence was cloned into PGL3 basic vector (Promega). Primers used were listed in Table1.

In vitro synthesis of antisense RNA probe

Antisense RNA probes were prepared by in vitro transcription according to the standard protocol. The following digoxigenin-labeled antisense probes were used: *c/ebp1*, *mpx*, *lyz*, *mfap4*, *csf1r*, *mpeg1.1*, *l-plastin.*

Whole-mount in situ hybridization (WISH)

Digoxigenin (DIG)-labeled RNA probes were transcribed with T7, T3 or SP6 polymerase (Ambion, Life Technologies, Carlsbad, CA, USA). Whole-mount mRNA in situ hybridization was performed as described previously(2). The probes labeled by DIG (Roche, Basel, Switzerland) were detected using alkaline phosphatase-coupled anti-digoxigenin Fab fragment antibody (Roche, Basel, Switzerland) with BCIP/NBT staining (Vector Laboratories, Burlingame, CA, USA).

MO and mRNA injection

The MO and mRNA were injected at the one-cell stage of the embryos. The MOs were designed and generated by Gene Tools, Philomath, OR, USA. MO sequences were shown in Table 2. Full-length capped mRNA samples were all synthesized from linearized plasmids by using the mMessagemMachine SP6 kit (Life Technologies-Ambion, Austin, TX, USA).

Sudan Black staining

The embryos treated with 4% paraformaldehyde (PFA) overnight at 4℃ were incubated with a Sudan Black (Sigma-Aldrich) solution for about 30 minutes to detect the granules of granulocytes. The detailed method was described previously(3). Staining was then observed under a microscope.

Cell collection and FACS analysis

Cell collection and FACS analysis were performed essentially as described(4). Wild type Tg(*mpx*:eGFP) and *irf2bp2b*$^{-/-}$//Tg(*mpx*:eGFP) embryos, as well as wild type Tg(*mpeg1.1*:eGFP) and *irf2bp2b*$^{-/-}$//Tg(*mpeg1.1*:eGFP) embryos were dissociated into single cells using 0.05% trypsin (Sigma) as previously described(5) at 48hfp. These dissociated cells were passed through a 40-μm mesh, centrifuged at 450g, and suspended in 5% FBS/PBS before addition of propidium iodide to a final concentration of 1 μg/ml for exclusion of dead cells. FACS analysis was based on forward and side scatter characteristics, propidium iodide exclusion and GFP fluorescence using a FACS Vantage flow cytometer (Beckton Dickenson). Wild type embryos (without GFP) were used as blank to determine the background values in GPF-controls.

H&E staining of paraffin sections

After being collected and fixed with 4% paraformaldehyde (PFA) overnight at 4 °C, the embryos were dehydrated by progressively higher concentrations of ethanol, substituted with

xylene, embedded in paraffin wax, cut into 3-5μm slices, for hematoxylin and eosin (H&E) staining. Then the samples were imaged under a light microscope (Nikon).

PH3 staining and TUNEL assay

Tg(*mpx*:eGFP) , Tg(*mpeg1.1*:eGFP), irf2bp2b$^{-/-}$//Tg(*mpx*:eGFP), and irf2bp2b$^{-/-}$//Tg(*mpx*:eGFP) embryos were collected at 48hpf and fixed in 4% paraformaldehyde. The fixed embryos were incubated with primary rabbit anti-phospho-histoneH3 (pH3; Upstate Biotechnology) and goat anti-GFP (Abcam) antibodies according to the manufacturer's protocol and subsequently stained with AlexaFluor-647 anti–rabbit and AlexaFluor-488 anti–goat secondary antibodies (Invitrogen). TUNEL assays were performed using the In Situ Cell Death Detection Kit and TMR Red (Roche Diagnostics) according to the manufacturer's recommendations. Images were taken using Olympus FV 1000 confocal microscopy equipped with the FV10-ASW version 3 software.

Retroviral transduction

The IRF2BP2 cDNA was inserted into pMSCV-neo vector. For retroviral transduction, plat-E cells were transiently transfected with retroviral vectors. 32Dcl3 Cells were transduced by spinoculation (1,300 g, 30℃, 90 min) in a retroviral supernatant supplemented with cytokines and 4μg/ml polybrene (Sigma). Transduced cells were selected by G418 treatment (800mg/ml, Sigma).

Quantitative RT-PCR

The quantitativePCR was carried out with SYBR Green Real-time PCR Master Mix (TOYOBO) with ABI 7900HT real-time PCR machine, and analyzed with Prism software. The primers used were listed in Table.

ChIP-PCR

For ChIP analysis, GFP or GFP-Irf2bp2b expressing embryos were harvested at 48hpf for brief fixation. Cross-linked chromatin was immunoprecipitated with anti-GFP antibody

according to the procedure described(6). The resultant immunoprecipitated samples were subjected to semiquantitative PCR using primer pairs (Table1).

Cell culture and Luciferase reporter assay.

HEK293T cells were maintained in DMEM (Life technologies, Grand Island, NY, USA) with 10% Fetal Bovine Serum (Life technologies, Grand Island, NY, USA). Plasmid transfection was carried out with Effectene Transfection Reagent (QIAGEN) according to manufacturer's instruction. For the luciferase reporter assay, cells were harvested 48 hours after transfection and were analyzed using the Dual Luciferase Reporter Assay Kit (Promega, Maddison, WI, USA), according to the manufacturer's protocols.

Western blot and Co-Immunoprecipitation assay

HEK293T cells, which had been transfected with plasmids for 48h, were washed with phosphate-buffered saline (PBS) buffer for 1 minute 3 times. Lysates were prepared using RIPA lysis buffer (Beyotime, Shanghai, China) with proteinase inhibitor (Roche, Basel, Switzerland), after shaking on ice for 30 minutes, the cells were harvested and centrifuged at 15,000 × g for 30 min. Rabbit anti-HA antibody (Santa Cruz) was mixed with the protein-G-agarose beads (30 μl) in the supernatant at 4 °C overnight. The beads were prepared by centrifugation and washed three times with RIPA lysis buffer. Proteins binding to the beads were eluted by adding 30 μl of 2× SDS sample buffer and analyzed by immunoblotting using anti-GFP antibody (Santa Cruz).

References

1. Xiao A, Wang Z, Hu Y, Wu Y, Luo Z, Yang Z, et al. Chromosomal deletions and inversions mediated by TALENs and CRISPR/Cas in zebrafish. Nucleic acids research. 2013 Aug;41(14):e141.
2. Thisse C, Thisse B. High-resolution in situ hybridization to whole-mount zebrafish embryos. Nature protocols. 2008;3(1):59-69.
3. Le Guyader D, Redd MJ, Colucci-Guyon E, Murayama E, Kissa K, Briolat V, et al. Origins and unconventional behavior of neutrophils in developing zebrafish. Blood. 2008 Jan 1;111(1):132-41.
4. Traver D, Paw BH, Poss KD, Penberthy WT, Lin S, Zon LI. Transplantation and in vivo

imaging of multilineage engraftment in zebrafish bloodless mutants. Nature immunology. 2003 Dec;4(12):1238-46.
5. Yan C, Huo X, Wang S, Feng Y, Gong Z. Stimulation of hepatocarcinogenesis by neutrophils upon induction of oncogenic kras expression in transgenic zebrafish. Journal of hepatology. 2015 Aug;63(2):420-8.
6. Hart DO, Raha T, Lawson ND, Green MR. Initiation of zebrafish haematopoiesis by the TATA-box-binding protein-related factor Trf3. Nature. 2007 Dec 13;450(7172):1082-5.